Arch Computat Methods Eng (2017) 24:397–422
DOI 10.1007/s11831-016-9164-5

ORIGINAL PAPER

Historical Origin and Recent Development on Normal Directional Impact Models for Rigid Body Contact Simulation: A Critical Review

Arnab Banerjee[1] · Avishek Chanda[1] · Raj Das[1]

Received: 7 November 2015 / Accepted: 6 January 2016 / Published online: 21 January 2016

Abstract The impact is one of the most abundant phenomena in the field of multi-body dynamics when two or more bodies come in close vicinity and depending on the interaction properties and geometry, all the interacting bodies experience certain impulsive force for an infinitesimal duration. Nowadays, impact modelling becomes an intrinsic part in the modelling of structural pounding, granular materials, crash and machinery analysis, robotics and bio-mechatronics applications. Since the time of Newton, numerous literatures have been published on the modelling of both normal and oblique contact phenomena. The scope of this critical review is limited to consolidate the existing knowledge on the computational model of normal directional impact on rigid bodies. The literature related to modelling of oblique impact, soft body impact, impact damage in composites and associated stress wave propagation are excluded from the scope of this critical review. Smooth and non-smooth mechanics are two schools of thought in simulating the normal directional impact. In this review, the shortcomings of all the classes of compliance and non-smooth models are analysed in the unified dimensionless frame-work to compare their response output with the conventional stereo-mechanical model. This review opens a new avenue for future researchers in selecting a proper contact formulation for specific application.

List of symbols

K	Stiffness of the linear spring
M	Mass of the impact
δ, δ_P, $\delta_{\max}$, x	Relative indentation, plastic deformation, and maximum penetration, dimensionless penetration
R_i, ΔR, L	Radius of impacting solids, radial clearance, length of cylinder joint
v	Poisson's ratio
E	Young's modulus
F, $F_{\max}$, $\tilde{F}$	Restoring force and the maximum possible force, dimensionless force
A	Impacting area
ξ, C	Damping ratio, coefficient of damping
t_h	Thickness of the spur gears
$\dot{\delta}_N^-, \dot{\delta}_N^+, \dot{\delta}, \dot{x}$	Pre-impact relative velocity, post-impact relative velocity, velocity during virtual penetration, dimensionless velocity during virtual penetration
ε_N	Coefficient of restitution
$\Lambda_N, \tilde{\Lambda}_N, \Lambda_{NC}, \Lambda_{NE}$	Impulse, dimensionless impulse, impulse in compression phase and impulse in restitution phase
$\Phi^+, \Phi^-, \Xi, \tilde{\Xi}$	Kinetic energy of pre-impact, post-impact, energy loss, and no dimensional energy loss
$t, \Delta T, \tau$	Time, total time for contact duration, non-dimensional time

✉ Arnab Banerjee
aban991@aucklanduni.ac.nz; abanerjee24@gmail.com

Avishek Chanda
acha553@aucklanduni.ac.nz; a.chanda91@gmail.com

Raj Das
r.das@auckland.ac.nz

[1] Department of Mechanical Engineering, The University of Auckland, 20 Symonds Street, Auckland 1010, New Zealand

1 Introduction

The impact can be defined as that phenomenon, when a system of two or more bodies comes in contact for a very short duration of time, resulting in different responses depending on the material property, the geometry of the concerned bodies and also their pre-impact conditions. The study of dynamic systems, comprised of more than one body, is known as the multi-body dynamics, where the interactions of the concerned bodies are influenced due to the presence of the kinematic constraints when an external force is applied. Thus, multi-body systems can be defined as those systems of multiple bodies where the relative motion of the system, due to the application of an external force, is constrained by the constituent kinematic pairs [1–3].

The forces, acting on the multi-body system, may include inertia or gravitational forces, state-dependent forces, concentrated forces or others and often result in impacting events [4–7]. The impact phenomenon may result in failure due to vibration, load propagation, fatigue, cracks, wear and other detrimental events leading to the inefficient functioning of the system. The pioneer works in this field can be found more than a century ago and still has a significant importance in the modern research and other engineering activities [8–13]. The applications of the multi-body dynamics and the impact phenomenon range from the modelling of the civil and infrastructural applications, such as, bridge segments [14–19] or closely spaced buildings [20–24] to the modelling of granular structures, like, sand, clay and others, i.e., in the simulation of the contact problem experienced in the Discrete Element Method [25–27]. Significant applications of the contact mechanics can be observed also in the crash analysis [28–30], parts of mechanical machines [31–34] and vehicle bridge interactions [4, 35–44]. In the modern days, the application field has even extended to the field of robotics [45–47], bio-mechatronics [48–52], simulating systems with Smoothed Particle Hydrodynamics [53–55], mesh-free method [56], the Material Point method, impacts on composite structures, such as, fibre metal laminates [57, 58] and many others.

The roots of multi-body dynamics lie in the classical methods that were used analytically and have grown to accommodate all the complex and modern technologies in engineering. In the present days, the most challenging aspect, for engineers, lies in the selection of the most suitable constitutive model for the impacting system under consideration, due to the influential geometries and kinematics of the bodies under impact [59–61]. The other challenges include estimation of the influential contact parameters [4, 62, 63] and the quantification of the energy transfer [64–66]. The problem, in choosing the idle model for simulating a particular response, becomes more intense due to the availability of various available methods, as illustrated in Fig. 1. The first ever method was proposed by Hertz [67, 68] based on the linear spring model and was completely elastic in nature, with no energy dissipation. Over the century, many other models have been developed, to achieve the desired coefficient of restitution, impulse and energy loss according to Newton's laws, leading to the different compliance models and non-smooth models, as shown in Fig. 1. There are two other finite element model

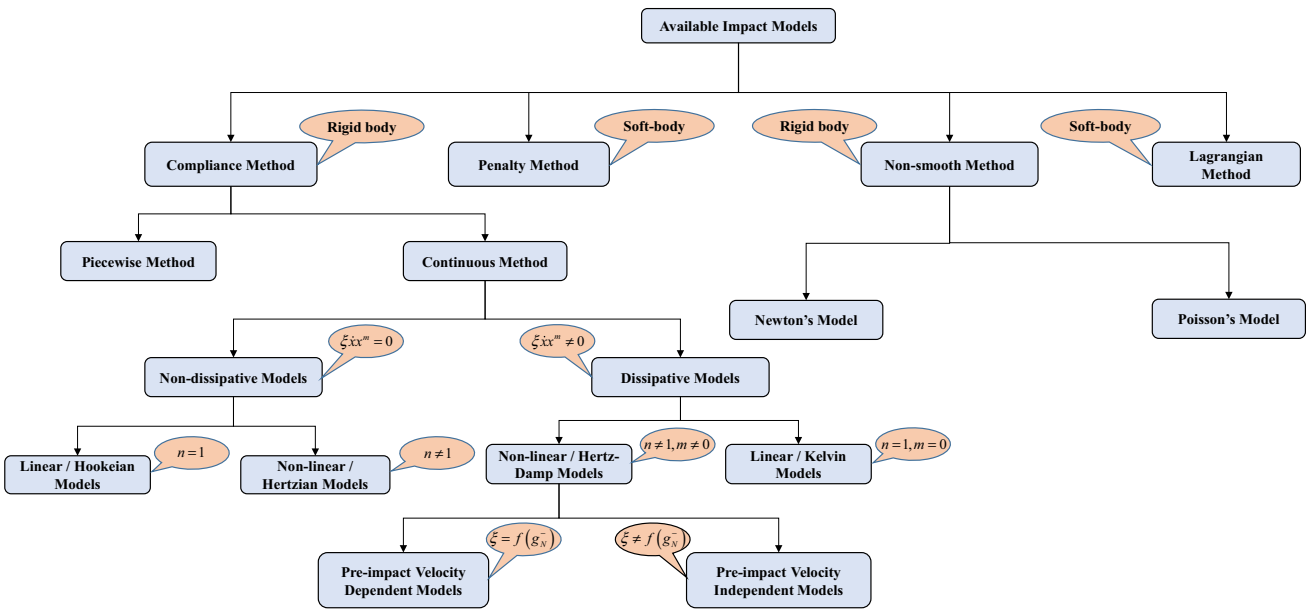

Fig. 1 Existing impact models

based approaches, employed by the Finite Element Analysis software Ansys [69], Abaqus [70, 71] and others, namely, the penalty method and the Lagrangian multiplier method [72]. These models work with the availability of multiple nodes only and are employed exclusively to formulate soft body impacts. Thus, the available impact models can be categorised as illustrated in Fig. 1. The use of the penalty method is computationally much simpler because, since, the contact force, being a continuous function of the indentation, the method is independent of the impulse dynamic calculation [73, 74]. However, there exists a few disadvantages as well. The main problem lies with the selection of the appropriate contact parameters for complex cases [75, 76] and also in the introduction of iterative high-frequency dynamics, which needs a significant reduction of step time, and thus, greatly increases the total simulation time [77]. Therefore, for analytical solutions of rigid bodies, this method is usually not used in the available literature.

The main disparity in the models lies in the identification of the contact points and the penetration of the bodies under impact. The geometric constraint-based models, determined through Lagrangian multipliers [78], the contacting points are co-incident [7]; whereas, a certain amount of penetration of the impacting bodies is allowed with the penalty method [79] and absolutely no penetration is allowed for the non-smooth one. One of the most important aspects of all the non-smooth and compliance models is that they belong to a system of rigid body impact. A body can be identified as a rigid body when the deformation experienced is negligible compared to that of the total dynamics [80]. The first ever experimental test was conducted by van Mier et al. [81] who analysed the response of an inverse pendulum, under impact, for different shapes of the impactor.

The phenomenon of impact can be briefly defined as the state when two bodies, in close proximity, approach each other with a relative velocity, called the pre-impact velocity, and collide resulting in the gradual reduction of the velocity. The velocity is nullified due to the work done by the force of contact, corresponding to the end of the compression stage with the maximum indentation. This marks the beginning of the expansion stage, where the energy, stored during the previous stage, drives apart the two bodies in contact. Subsequently, some energy, due to the internal damping [82], is lost through vibrations, heat, sound and in other forms [83]. Perfectly elastic collisions between two bodies have also been observed to dissipate energy, due to the transformation of the initial kinetic energy into internal vibrations, after contact [84]. Thus, initially proposed elastic models needed to be evolved in order to accommodate the energy dissipating phenomenon. Although, the energy dissipating impact model has experienced many evolutions, the coefficient of restitution is still the most important aspect which governs the energy dissipation. This can be defined as the ratio of the post-impact relative velocity to the pre-impact relative velocity of the body under impact. The coefficient of restitution can be generally defined as a constant of proportionality between the two relative velocities and depends on the geometry of the body concerned, the pre and post-impact velocities, friction and temperature of the system [85–88]. It may also depend on the relative impulse experienced by the system under impact. Extensive studies have been carried out in the recent times by Machado et al. [63] and Alves et al. [7] elaborating on the different important models available and how they individually vary with the experimental results [89] and also compare with the Hertz model [67, 68]. Both the works were concerned mainly with the models based on the compliance method with no emphasis on the non-smooth method. Also, the comparison between all the available models was not performed extensively in any of the available literatures of recent times.

This work focuses on critically reviewing all the available and applied impact analysis methods, which include both compliance and non-smooth methods. The evolution of the each method and the available models under each category are detailed and compared extensively. In order to compare the related models, all the available models are non-dimensionalised so that they can be compared accurately on a same dimensionless field. Two most important post-impact responses, namely, the post-impact velocity and the impulse due to impact will be extensively elaborated and compared for each model, unlike the other available literatures. This work concentrates only on the available models on the normal response, which can be defined as the situation when the centre of masses of the two impacting bodies lie on the perpendicular drawn from the impacting surfaces of the contact points, experienced by the multi-body system under impact. The oblique impact and the effect of friction are excluded from the scope of the review. The formulations and frame work created are exclusively dependent on the rigid body analysis and thus only the methods related to the rigid body contact are considered. The Lagrangian multiplier and the penalty methods, being used for soft bodies only, lie outside the scope of this review. The main objective of this work is to provide users with a common platform, where they can easily compare and select the most suitable impact model and also to consolidate the existing knowledge of contact models with their advantages and disadvantages.

2 Evolution of the Compliance Models

The fundamental of contact kinematics, between two potentially impacting bodies, lies in the evaluation of the relative pre- and post-impact velocities, the possible contact points and the distance between the two points [6, 90,

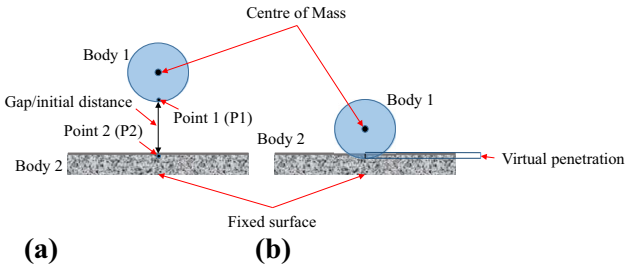

Fig. 2 Compliance model based illustration of **a** two bodies in rest and **b** the bodies under impact

91]. Figure 2a illustrates two bodies in the state of rest with two potential contacting points P1 and P2 with a gap between them. The motion of all the bodies in a multi-body system is constrained by the relative velocity of the potential impacting points and the also by the distance between them [63]. When the compliance model is considered, the bodies after impact behave in a way which is shown in Fig. 2b and experiences a certain amount penetration [77, 92–96].

Any impact model consists of two phases, the approach phase when the bodies approach each other resulting in contact and the restitution phase, which starts after the pre-impact relative velocity becomes zero and the bodies start to separate from each other. The compliance based models provide some approximated force-penetration curves for simulating the contact phenomenon. The models are very efficient and have the ability to handle the impacts, endure the contacts under all conditions and also have the capability of transformation to and from the state of impact [97]. The system of collision and the effects on the bodies have been extensively modelled, for more than one century, by idealising the entire system into having spring-damper systems on the surface of the bodies under impact. The stiffness of the spring-damper element and the amount of deflection can be calculated with respect to the relative indentation, surface geometries and properties of the constituent materials. The compliance model is very easy and simple to be implemented in the generalised impact cases because the contact force is a function of the indentation in between the bodies in contact. Various compliant models have been proposed till the present time and they include both completely elastic and energy dissipating models [7, 63, 98].

2.1 Compliance Elastic Models

The elastic compliance models are used to simulate the elastic collision, where no energy dissipation takes place during impact. Thus, theoretically the amount of energy conserved due to impact is completely transferred into the impacting bodies, which bring them apart. The pioneer in the study of contact kinematics was Hertz [67, 68], who studied the effects due to contact of two perfectly elastic bodies, back in 1881 [99]. This theory, famous as the Hertzian contact theory, was invented while studying the fringes of the optical interface in between the two lenses and the possible deformation of the surfaces of the lenses due to contact [82]. The law proposed by Hertz can be expressed as:

$$F = K\delta^n \tag{1}$$

where, $n = 3/2$, n being the non-linear power exponent, F is the contact force, δ stands for the indentation experienced and K represents the parameter for contact stiffness. The main feature of the model is the dependency of K on the material properties and geometry of the surfaces in contact [100]. Thus, the stiffness parameter varies with the variation in the geometry of the impacting surfaces. Goldsmith [82] defined the stiffness parameter for two spherical bodies (1 and 2), under impact, to be:

$$K = \frac{4}{3(\sigma_1 + \sigma_2)}\sqrt{\frac{R_1 R_2}{R_1 + R_2}} \tag{2}$$

where, the two spheres were isotropic in nature with radii R_1 and R_2. σ_1 and σ_2 are the parameters dependent on the material of the bodies and $\sigma_i = (1 - v_i^2)/E_i$ with $i = 1, 2$, representing the two contacting bodies, and with E_i and v_i being Young's modulus and Poisson's ratio respectively. The stiffness parameter changes when the two concerned impacting bodies become a sphere and a plane and can be stated as:

$$K = \frac{4}{3(\sigma_1 + \sigma_2)}\sqrt{R_i} \tag{3}$$

where, i again varies between 1 and 2 and R_i is the radius that is positive in the case of convex surfaces and negative for the concave ones [63]. This model has been extensively used both directly and in the modified form thus forming the platform for the numerous variants. The Hertzian theory was utilised directly for simulating the human knee as a multi-body system with the tibiofemoral and patellofemoral joints working as two separate bodies under contact [101]. One of the main disadvantages of the Hertzian model is its inability to evaluate the plastic deformation experienced by the bodies under high-velocity impact. Goldsmith [82] proposed a model, modifying the Hertz model, which accommodated the plastic deformation or indentation during the restitution period. The model can be stated as:

$$F = F_{\max}\left(\frac{\delta - \delta_P}{\delta_{\max} - \delta_P}\right)^n \tag{4}$$

where, δ_P stands for the permanent indentation experienced by the bodies due to impact, $F_{\max}$ represents the maximum possible force at the contact, δ is the indentation

experienced due to impact and δ_{max} is the maximum possible indentation that the bodies can experience due to impact.

The application of the contact model into a core mechanical field was done by Yang and Sun [102], who applied a linearised form of the Hertzian model for evaluating the dynamics experienced by the spur gears. The model can also be termed as a linear spring model and can be stated as:

$$F = K\delta \tag{5}$$

where, the symbols represent the same. The contact stiffness parameter, depending on the properties of the constituent material, was given as:

$$K = \frac{\pi E t_h}{4(1-\nu^2)} \tag{6}$$

where, t_h stands for the tooth thickness of the spur gears and ν and E represent Poisson's ratio and Young's modulus respectively. This linear model was considered in other studies as well, which include a study on the impact of a journal bearing system by Dubowsky et al. [103] and that on numerical modelling of granular structures by Cundall et al. [104]. The work on granular structures was the first ever application of the evolving Hertzian contact model in Discrete Element Method (DEM). The model proposed for monitoring the granular elements of DEM, for the contact of each particle, with the help of the computer program BALL, is:

$$F = K\Delta n = K\delta \tag{7}$$

where, the $\Delta n = \nu \Delta T$ represents the indentation of the model depending on Poisson's ratio (ν) and the change in time (ΔT).

Another limitation of the Hertzian contact model is its inability to evaluate the stiffness parameter for bodies experiencing contact along a line or a surface because it works only with the contact points. The model holds good only when the points of contact are known [105, 106]. Thus, for rectangular or cylindrical contacts, the Hertzian model fails to perform. This shortcoming was addressed by Brandlein et al. [107], through various theoretical and empirical investigations. The model proposed can be written as:

$$F = K\delta^n \tag{8}$$

where, $n = 1.08$ and the stiffness parameter, K, is independent of the radii of the bodies under impact and depends only on the length of the contact. Other studies have also used the same model for simulating the contact along a surface or a line for a multi-body system comprising of an infinitely long cylinder, in roller bearings [108].

Further studies led to the understanding of more weaknesses in the Hertzian model, leading to the development of new models. The Hertzian model works efficiently for impact cases with non-conformal points assuming that the contacting area is smaller than the radii of the contacting surface's curvature [109]. Thus, for cases with conformal points of contact, the model fails and studies have shown that the contacts could be 25 % stiffer than that evaluated using Hertzian model [110]. Thus, the Hertzian model was further extended by Liu et al. [111] for simulating cylindrical joints particularly for models with small clearances, since the Hertzian contact is valid only for models with large clearances and comparatively less loads [103, 112]. The proposed model can be represented as:

$$F = \frac{\pi E^* L \delta}{2}\left(\frac{\delta}{2(\Delta R + \delta)}\right) \tag{9}$$

where, L represents the length of the cylinder joint, ΔR denotes the radial clearance, δ is the relative indentation experienced by the bodies and E^*stands for the effective modulus that is given as:

$$E^* = \left(\frac{1-\nu_1^2}{E_1} + \frac{1-\nu_2^2}{E_2}\right)^{-1} \tag{10}$$

Liu et al. [113] extended their own work to formulate a similar model for spherical joints and it can be represented as:

$$F = \frac{KE^*\delta}{2R_2} \tag{11}$$

where, R_2 represents the depth of the spherical cavity and the other symbols denote the same as those of Eq. (9). Both the models, Eqs. (9) and (11), presented by Liu et al. [111, 113] can be denoted as a linear spring model, with δ being the only variable and the other terms, being constant, can be idealised as the stiffness parameter K.

2.1.1 Contact area Dependent Models

Unique models, based on the linear Hertz approach, was also proposed by Luo and Nahon [114]. This model was dependent on the area of the contacting geometry and an algorithm was used to find the variations in shape coefficient, contact area and penetration distance, in the case of polyhedral bodies, under impact. The model was exclusively based on the distinction between the interference geometry and the geometry of the true contacting point and thus, a line body and another face contacting body were selected. The model proposed was [114]:

$$F = 2E^* \frac{A}{\pi r_a}\delta \tag{12}$$

where, A is the impacting area and r_a is the average radius from the centre of the polygon. This model was further extended by the same authors to propose an overlapping

polyhedral contact models [115]. The extended model can be represented as:

$$F = \gamma \pi E^* \frac{A'}{\tau'_{\max}} \delta_{\max} \tag{13}$$

where, A' stands for the contact area, during impact, when the polygon, which is overlapping, matches with the other contact polygon, γ is the case coefficient that is dependent on the specific contact case, $\tau'_{\max}$ is the shape coefficient of the overlapping polygon and $\delta_{\max}$ denotes the maximum possible indentation.

The Hertzian model has been extensively evolved, in order to make the use plausible in all fields. Hippmann [95] proposed that the problem faced by Hertz's law, when the contact area seizes to be a point, can be neglected by considering an elastic foundation, that converts the surface into polygonal meshed elements. Incorporation of the Hertz's law based models into computationally efficient methods have been performed in many studies, especially for modelling the knee joints [116, 117] and also for the mathematical wear modelling [118]. In spite of all the advancements, the elastic model still had the greatest drawback of not being able to accommodate the energy dissipation which is inevitable in many practical fields. Thus, models, accommodating the dissipation of the impact energy, were obvious to follow.

2.2 Compliance Energy Dissipating Model

Studies showed that energy dissipation, during the compression and expansion stages of the contact, is always experienced in the practical field. Thus, the Hertzian contact model and the ones evolved from it failed to accommodate this dissipation criterion, which characterises the events of a mechanical structure under impact [63]. This realisation led to the development of contact models accommodating energy dissipation and the Kelvin and Voigt model was the first ever dissipating contact analysis model [82]. This model was followed by many other models with modifications being made even in the present time. The proposed models that accommodate the dissipative energy can be broadly classified into continuous models and piece-wise models. This part of the review categorises the dissipative models into the two broad classes chronologically, so that a distinction can be inferred in both simulation and output.

2.2.1 Continuous Model

The models based on the contact forces are known as the continuous models, where the contact phenomena is modeled as a continuous forcing function [7]. These models are dependent on a continuous function throughout the compression and expansion stages. The continuous models can be further divided into two types, namely, the linear model ($n = 1$, $m = 0$) and the non-linear model ($n \neq 1$, $m \neq 0$). This section reviews all the available continuous models of both Kelvin and Hertz-damp elements categorically and chronologically.

2.2.1.1 Linear (Kelvin) Model

The first ever energy dissipative model in contact mechanics was the Kelvin–Voigt's approach [82], which can be stated as:

$$F = K\delta + C\dot{\delta} \tag{14}$$

where, the initial term of the right-hand side (RHS) of the equation represents the linear force component in the elastic state and the second half of the RHS corresponds to the energy dissipative part of the contact. The term C, in Eq. (14), represents the coefficient of damping, δ is the indentation experienced and $\dot{\delta}$ is the relative velocity, during impact, in the normal direction. This model opened new dimensions for researchers and extensive studies on the evaluation of the contact forces between bodies [103, 119–122], dynamic simulations of planar mechanical structures [123], simulation of flexible multi-body systems [124], vehicle road interaction analysis [35, 125, 126] and others followed. In spite of the extensive usage, the studies indicated that further evaluation of the model was required in order to efficiently predict the realistic response of a system under impact. The limitations associated with the models included the miss-representation of the overall non-linear response because of the linear elastic term. The discontinuity of the contact force, at the beginning of the impact, makes the penetration zero at the end of the restitution period along with negative contact force and contact velocity and the presence of the constant damping coefficient throughout the impacting period [127].

These issues led to further development of the impact model and thus many authors have proposed different models, which are both pre-impact velocity dependent as well as independent, leading to the evolution of the Kelvin and Voigt model. Anagnostopoulos [20] modified the Kelvin and Voigt's model to propose a model that can be used for studying the pounding of adjacent buildings, during severe earthquakes. The model proposed was:

$$F = K\delta + C\dot{\delta} \tag{15}$$

where, $C = 2\xi\sqrt{KM} = 2\xi\omega$ and $C = 2(\ln \varepsilon_N)\sqrt{KM}$, with ξ being the damping ratio and ω is the natural frequency. The structural damages and subsequent collapses, of the buildings under impact, were the main modelling aim of the work and they were modelled by idealising each structure as a single degree of freedom system. It was observed that the response substantially increases at the

end-structures; whereas, an opposite trend is observed at the interior parts of the system.

Another modified linear Kelvin element model was proposed by Goyal et al. [128, 129] in 1994 for simulating the dynamics of the unconstrained rigid bodies experiencing interactions. The main aim of the authors was to run a computer simulation of the motion of the rigid bodies under impact and hence, proposed a contact model to be:

$$F = K\delta + C\dot{\delta} \tag{16}$$

where, $C = \xi/2M\omega_N$ and $\varepsilon_N = e^{-\left(\frac{4\xi}{\sqrt{1-\xi^2}}\right)\tan^{-1}\left(\frac{\sqrt{1-\xi^2}}{\xi}\right)}$. The value of ξ can be calculated from the implicit equation of ε_N and replaced in the equation of C to find the required values. The concept of soft contact was used in formulating the equations for the rigid body contact, in order to make the computational model equipped with multiple simulations. Brogliato [100] modified the model proposed by Goyal et al. [128, 129] in order to address the errors, such as, different coefficient of restitution in the output, a different impulse from what is expected and others, found in the later model. There was only one small modification in the model, where the force equation was the same as Eq. (16), with the value of the coefficient of restitution being:

$$\varepsilon_N = e^{-\left(\frac{2\xi}{\sqrt{1-\xi^2}}\right)\tan^{-1}\left(\frac{\sqrt{1-\xi^2}}{\xi}\right)} \tag{17}$$

This model was found to have much better responses of bodies under impact. The relation of the coefficient of restitution and the damping ratio of both the models proposed by Goyal and Brogliato are given in Fig. 3.

All the models that have been detailed in this section have one thing in common; the force is equal to zero when the gap between the bodies is greater than zero. Thus, it can be inferred that all the models work only when the gap becomes less or equal to zero.

2.2.1.2 Non-Linear (Hertz-Damp) Model Although many models were proposed based on the linear kelvin element, the models lacked realistic and physical approach. This requirement led to the inclusion of the non-linear element into the linear equation of Kelvin. Thus, Hunt and Crossley [65], were the pioneers in incorporating the non-linear Hertz element into the Kelvin and Voigt's model. This kind of energy dissipating models fall under the category of Hertz-damp models and have been observed to be usually of two types, namely, pre-impact velocity dependent models and pre-impact velocity independent models. This part of the review concentrates on the available Hertz-damp models along with the detailed chronological discussion of their two different types.

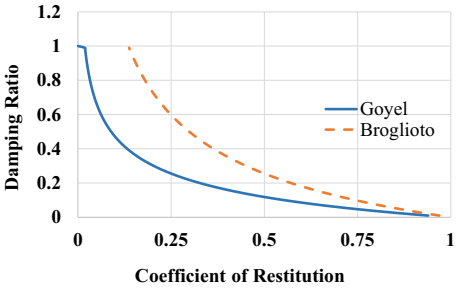

Fig. 3 Relationship between the damping ratio and the coefficient of restitution for the models proposed by Goyal [128, 129] and Brogliato [100]

- Pre-impact velocity independent models.

Continuous evolution of the contact model led to the development of the Hertz damp model. Kuwabara et al. [130] proposed the first Hertz-damp model, which is independent of the pre-impact velocity of the colliding bodies. The model was used to predict the coefficient of restitution for two colliding spheres and can be represented as:

$$F = K\delta^n + C\delta^m\dot{\delta} \tag{18}$$

where, the indices $n = 3/2$, $m = 1/2$ and C can be calculated from:

$$C = \frac{4D}{5}\left(R_{eff}\right)^{1/2}$$
$$D = \frac{3\left(1-\sigma_1^2\right)\left(1-\sigma_2^2\right)}{4E_1E_2} \quad \text{and} \quad R_{eff} = \frac{R_1R_2}{R_1+R_2} \tag{19}$$

Tsuji et al. [131] further expanded the contact model for the numerical simulation of discrete, non-cohesive and spherical particles for plug flow. The Lagrangian numerical method was utilised for the analysis of the entire structure and a new model was used to model the interaction between the spherical particles. The model proposed was:

$$F = K\delta^n + C\delta^m\dot{\delta} \tag{20}$$

where, $n = 3/2$, $m = 1/4$, $C = \alpha\sqrt{MK}$ and α is an empirical constant which is directly related to the coefficient of restitution. The relation between the two is given in Fig. 4 and the value of α can be directly derived for a known value of the coefficient of restitution (ε_N).

Lee and Herrmann [132] modified the velocity independent, non-linear model in order to make it more realistic when compared to the practical cases. They simulated piles which can be generated due to avalanches and the model can be represented as:

$$F = K\delta^n + C\delta^m\dot{\delta} \tag{21}$$

where, $n = 3/2$, $m = 1$, $C = \xi M_{eff}$ and the value of ξ was considered to be 5×10^2. Brilliantov [133, 134] used this type of model and further modified it in order to simulate a model for colliding granular gaseous materials and for

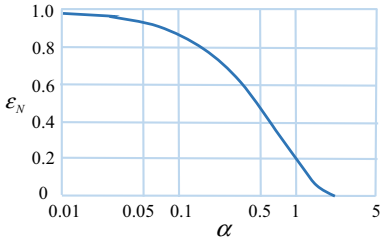

Fig. 4 The empirical relationship betweenαandε_N [131]

calculating the coefficient of restitution. The proposed model was:

$$F = K\delta^n + C\delta^m\dot{\delta} \tag{22}$$

where, $n = 3/2$, $m = 1/2$, $C = K(3\eta_2 - \eta_1)^2(1 - v^2)(1 - 2v)/2(3\eta_2 + 2\eta_1)Ev^2$ and η represents the constant of viscosity, v is Poisson's ratio and E is Young's modulus. This model paved the way for the incorporation of the viscous constant into the impact models and many other studies including the one conducted by Schwager et al. [135] used the viscous constant in the respective impact models. The last evolved pre-impact velocity independent Hertz-damp model was proposed by Bordbar and Hyppanen [136], who were also influenced by Brilliantov's modification. The main aim of the study was to provide an accurate value of m, in order to efficiently model the collision between viscoelastic spheres of different sizes. The model proposed can be demonstrated as:

$$F = K\delta^n + C\delta^m\dot{\delta} \tag{23}$$

where, $n = 3/2, m = 0.65, C = K(3\eta_2 - \eta_1)^2(1 - v^2)(1 - 2v)/2(3\eta_2 + 2\eta_1)Ev^2$. Various linear and non-linear type impact force models and the coefficient of restitution, in the normal direction, was carried out with the new model in order to validate and confirm its working efficiency. Till this stage of the review, it can be said that the impact model has evolved extensively from the linear Hertz model to energy dissipating models, also called the Hertz-damp models. However, a very important aspect of any multi-body system, the pre-impact velocity, has not yet been considered in any of the proposed models.

- Pre-impact velocity dependent models.

The pre-impact velocity, which is the velocity with which the bodies approach each other, has considerable potential to change the response of the entire multi-body system, under impact. Studies and experiments have shown that the change in the pre-impact relative velocity greatly affects the response of the impacting systems. Thus, it was necessary to propose impact analysing models dependent on the pre-impact velocity of the bodies, under study. Hunt and Crossley [65] were the first to propose a model which depended on the pre-impact relative velocity of the system. The authors placed an argument that during the case of vibro-impact, the coefficient of damping must be proportional to the spring force's power and they even proved that the linear approach used by the Kelvin and Voigt does not accommodate the physical nature of the transferred energy at the time of impact. They proposed a model combining the non-linear viscoelastic component and the linear Hertz law, which can be stated as:

$$F = K\delta^n + C\delta^m\dot{\delta} \tag{24}$$

where, $n = m = 3/2$ and $C = 3(1 - \varepsilon_N)K\Big/2\dot{\delta}^-$, $\dot{\delta}^-$ is the pre-impact relative velocity and K is the parameter of the contact stiffness having the same value as the one proposed by Hertz. This model paved the way for realistic estimation and calculation of the contacting parameters and was subsequently used in many studies due to its simple implementation [137]. The introduction of a similar model, based on the one proposed by Hunt and Crossley, was also proposed for simulating robotic systems by Marhefka and Orin [46], paving the way for the application of a unique non-linear contact model into the field of robotics. In spite of its great significance, studies have shown that this proposed model works efficiently only for those cases where the coefficient of restitution is very high [46, 138, 139].

The velocity dependent model proposed by Hunt and Crossley [65] was modified by Herbert and McWhannell [140], who incorporated the coefficient of restitution into the model. Thus, the authors made the response of the multi-body system dependent on the coefficient of restitution and the model proposed by them was:

$$F = K\delta^n + C\delta^m\dot{\delta} \tag{25}$$

where, $n = m = 3/2$ and $C = 6(1 - \varepsilon_N)K/((\varepsilon_N - 1)^2 + 3)\dot{\delta}^-$. The model was established by combining the equations of motion in the dynamic state with the model proposed by Hunt and Crossley and was successfully used in a few studies [63, 141]. This model had a disadvantage of producing a higher amount of energy dissipation than usual and this led to further modification by Lee and Wang [86]. Another concern was to accommodate the expected boundary conditions, which included no damping force and maximum relative indentation at zero. The model proposed by them was the same with only a different damping coefficient, C. The model proposed can be shown as:

$$F = K\delta^n + C\delta^m\dot{\delta} \tag{26}$$

where, $n = m = 3/2$ and $C = 3(1 - \varepsilon_N)K\Big/4\dot{\delta}^-$. This model was established by accommodating dynamic modelling along with the analysis of the mechanisms in the

presence of intermittent contacts. This model was also used by Yigit et al. [142] for comparing impacting spring-dashpot systems, in order to simulate a flexible beam experiencing radial rotation. A further modification was carried out to make the model more realistic, leading to the development of another evolved model by Lankarani and Nikravesh [143]. This model also had a similar modification in the formula for calculating the coefficient of damping and can be given as:

$$F = K\delta^n + C\delta^m\dot{\delta} \tag{27}$$

where, $n = m = 3/2$ and $C = 3\left(1-\varepsilon_N^2\right)K\Big/4\dot{\delta}^-$. The new expression for the damping coefficient was formulated through relating the loss in kinetic energy due to the impact and the internally dissipated energy due to damping. The model proposed by Lankarani and Nikravesh was found to be satisfactory for cases involving general mechanical contacts and especially for those cases where the coefficient of restitution values which are closer to unity, i.e., the amount of energy dissipation is comparatively less than the maximum amount of elastic energy absorbed during the impact [63, 143]. Studies demonstrated that the coefficient of restitution is the main influencing factor for the response of the multi-body system, especially for impacts under low velocities [144]. This dependency of the system's response lead to the application of the model in many studies and in different fields [145–150] including the extension of the work to incorporate the plastic deformation, for high-velocity impact [151]. Muthulumar and DesRoches [150] used the model proposed by Lankarani to simulate pounding experienced in structures, for the first time.

The limitation of the velocity dependent non-linear models, presented so far, is that they work efficiently only for those impact cases, where the contact area is significantly smaller when compared to the dimensions of the bodies under contact. Gonthier et al. [138] were the first to propose a model where the large contacting areas can be accommodated. The proposed model can be represented as:

$$F = K\delta^n + C\delta^m\dot{\delta} \tag{28}$$

where, $n = m = 3/2$, $C = K\left(1-\varepsilon_N^2\right)\Big/\varepsilon_N\dot{\delta}^-$ and the damping ratio K is dependent on the contact area. This model was observed to be superior to the other proposed velocity dependent impact models, because solving Eq. (28) gives the exact solution desired for the dynamic contact cases. For a perfectly elastic contact ($\varepsilon_N = 1$) the damping factor assumes a zero value and is infinite for a purely inelastic contact ($\varepsilon_N = 0$). All these unique features were not observed in any of the models that have been proposed so far.

In spite of obtaining an exact solution, the model proposed by Gonthier et al. [138] and all others neglected the effect of the external forces, such as gravity, on their equation of motion, because the contact force usually dominates the impact process. Zhang and Sharf [152] proposed another unique compliant model where the coefficient of damping could be found directly from an implicit solution, making the value more accurate and logical. The proposed model was same as most of the other models, with a unique expression for the coefficient of restitution. The model can be given as:

$$F = K\delta^{3/2} + C\delta^{3/2}\dot{\delta} \tag{29}$$

where, $n = m = 3/2$ and $K\ln((C\dot{\delta}^- + K)/(-C\varepsilon_N\dot{\delta}^- + K)) = 2C\dot{\delta}^-\varepsilon_N$, which is an implicit expression, used for finding the value of C. In order to develop a stronger relation among the energy dissipated during contact, the impact parameters and the coefficient of restitution, Zhiying and Qishao [153] proposed a further modified model, that can be given as:

$$F = K\delta^n + C\delta^m\dot{\delta} \tag{30}$$

where, $n = m = 3/2$ and $C = 3K(1-\varepsilon_N^2)e^{2(1-\varepsilon_N)}/4\dot{\delta}^-$. The impact model experienced further modifications, all having the same aim of getting the same coefficient of restitution as the initial, equal amount energy dissipation when compared to the practical processes and the desired impulse due to impact. This led to a more modified model by Ye et al. [154], who proved that the model used by Muthukumar and DesRoches was not suitable for analysing the pounding experienced by structures, since the dependency on the stiffness of the spring, the relative approach velocity of two colliding bodies and the coefficient of restitution are incorrect and results in wrong pounding simulation. The new model proposed by the authors, for simulating poundings in structural engineering, can be given as:

$$F = K\delta^n + C\delta^m\dot{\delta} \tag{31}$$

where, $n = m = 3/2$ and $C = 8K(1-\varepsilon_N)\Big/5\varepsilon_N\dot{\delta}^-$. The model was also verified through numerical analysis and the assumption of the damping constant was found to be more accurate. Flores et al. [155] used the same model, as the one proposed by Ye et al. [154], for simulating the contact between soft materials. Luo and Nahon [115] proposed a further modified model in order to simulate two polyhedron objects, where it considers the explicit distinction in between the interference geometry and the true contact geometry. The model proposed by these authors can be represented as:

$$F = K\delta^n + C\delta^m\dot{\delta} = K\delta^n\left(1 + C'\dot{\delta}\right) \tag{32}$$

where, $n = m = 3/2$, $C' = C/K$ and $(1+\varepsilon_N)C'\dot{\delta}^- = \ln\left(\left(1 + C'\dot{\delta}^-\right)\Big/1 - C'\varepsilon_N\dot{\delta}^-\right)$. The proposed model was validated using available analytical models, finite element

analysis and also by using experimental data. Further modifications were made by Gharib and Hurmuzlu [156] in order to formulate a new impact model for simulating impacts with a low coefficient of restitution. The proposed model was:

$$F = K\delta^n + C\delta^m\dot{\delta} \tag{33}$$

where, $n = m = 3/2$ and $C = K\Big/\varepsilon_N\dot{\delta}^-$. Correlations between the compliance method (contact stiffness) and the impulse-momentum based method (coefficient of restitution) were presented by the authors and a numerical simulation was also carried out in order to validate the analytically obtained model. Another significant model was proposed by Khatiwada et al. [157], very recently, where the authors modified the model proposed by Hunt and Crossley, for retrieving the responses of building pounding, by proposing a more suitable damping coefficient. The model proposed by the authors can be stated as:

$$f = K\delta^n + C\delta^m\dot{\delta} \tag{34}$$

where, $n = m = 3/2$ and $(1 + \varepsilon_N) = (K/C\dot{\delta}^-)\ln|((K/C\dot{\delta}^-) + 1/((K/C\dot{\delta}^-) - \varepsilon_N)|$. The value of the coefficient of damping, for this model, was found to be exactly the same as the one derived from the relation proposed by Luo et al. [114, 115] and thus gives an exactly similar response. These models have led to the development of many unique methods to calculate the response of a multi-body system under response. The available compliance based models, being the mostly used, play a significant part in the study of impacting systems, for understanding the different pre- and post-impact phenomena as well as that occurring during the impact, in various fields of engineering [13, 158–174].

2.2.2 Piecewise Model

The continuous models have proved their limitations in calculating the exact same coefficient of restitution and the same impulse after completion of the contact phase. This led to the development of an alternative impact model considering for the Hertz-damp element, which was known as the piecewise method or the multi-linear gap element. Valles and Reinhorn [175, 176] were the first to propose a piecewise model for calculating the response of the bodies under impact. This model experiences energy dissipation in two different contact phases and thus, consists of two separate contact stiffness parameters, without any damping constant. The model can be represented as:

$$F = \begin{cases} K_1\delta & \left(\dot{\delta} > 0\right) \\ K_2(\delta - \delta_P) & \left(\dot{\delta} \le 0\right) \end{cases} \tag{35}$$

where, δ_P is the remaining displacement experienced by the model, as shown in Fig. 5. This model was proposed for calculating the response due to pounding between adjacent buildings. The coefficient of stiffness was assumed to be less during the approach period (K_1), with increasing compression force, and to be large for the expansion phase (K_2), with decreasing compression force. It is to be noted that this model is a linear model as can be observed from Fig. 5.

This model was further modified by Jankowski, who incorporated the non-linear damping element, for the purpose of simulating the results of structural pounding, induced by earthquakes. The proposed model can be given as:

$$F = \begin{cases} K\delta^{3/2} + C\delta^{1/4}\dot{\delta} & \left(\dot{\delta} > 0\right) \\ K\delta^{3/2} & \left(\dot{\delta} \le 0\right) \end{cases} \tag{36}$$

where, $C = 2\xi\sqrt{KM_{eff}}$ and $\xi = \sqrt{5}\left(1 - \varepsilon_N^2\right)\Big/2\pi\varepsilon_N$ when the relationship between the rebounding and approaching velocities and $\xi = 9\sqrt{5}\left(1 - \varepsilon_N^2\right)9\sqrt{5}\left(1 - \varepsilon_N^2\right)2\varepsilon_N(\varepsilon_N(9\pi - 16) + 16)$ when the restitution period's relative velocity and also the relationship between the post and pre-impact velocities are considered. These models described the contact phenomenon more practically and the change in phase can be observed from the entire response of the bodies under impact. At this point of the review, it can be concluded that, all the available continuous and piecewise linear and non-linear models, under the compliance based approach, have been summarised and chronologically categorised. However, the main existing problem lies with the time lag experienced during simulation, a phenomenon which is not practical for hard body and instantaneous contacts.

3 Non-Smooth Method

The main drawbacks of the compliance method based models are the time lag experienced, making it unsuitable for instantaneous contacts, and the compulsion of the

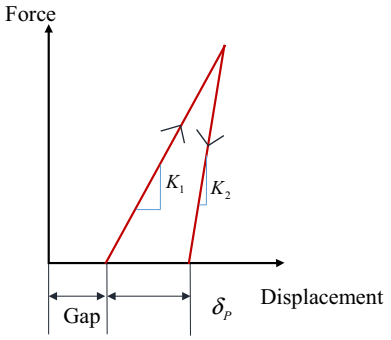

Fig. 5 A typical response of the Valles and Reinhorn model [23, 175]

velocities and positions to be continuous with time. This problem can be addressed by the non-smooth techniques where neither the model experiences any time lag nor there is any compulsion of smooth time evaluation of the velocity and position. The linear complementarity is the most used method for solving a set of linear algebraic equation$y = Ax + B$ in the non-smooth frame-work [177]. Here, both y and x are unknown, but A and B are known and there are two additional conditions, $y^T x = 0$ and $y, x \geq 0$. The method works with the assumption that the contact bodies are rigid in nature and solves the impact problem by utilising the unilateral constraints. The linear complementarity problem solves the resulting impulses, due to contact, thus, preventing the penetration phenomenon using an explicit formulation, based on unilateral constraints, between the rigid bodies in contact [178]. Another important assumption, for the method, is the consideration of no attraction between the bodies, under impact, signifying the complete absence of the impulse when there is no contact. The basic concept behind the complementarity problem is that the respective impulses of the constraints are zero when the relative kinematic is zero and vice versa [63, 179].

The evolution of the non-smooth method came from the Stereo-mechanical approach, which uses the concept of momentum conservation during the time of the collision to predict the post-impact velocities of the two masses, under impact [23]. The velocities can be given as:

$$\begin{aligned} \dot{\delta}_1^+ &= \dot{\delta}_1 - (1+\varepsilon_N)\left(\frac{m_2}{m_1+m_2}\right)\left(\dot{\delta}_1 - \dot{\delta}_2\right) \\ \dot{\delta}_2^+ &= \dot{\delta}_2 - (1+\varepsilon_N)\left(\frac{m_1}{m_1+m_2}\right)\left(\dot{\delta}_2 - \dot{\delta}_1\right) \end{aligned} \tag{37}$$

where, $\dot{\delta}_i (i = 1, 2)$ is the initial velocity of the ith body, $\dot{\delta}_i^+$ represents the post-impact velocity of the ith body, m_i is the mass of the ith body and ε_N is the coefficient of restitution in the normal direction. This method does not provide any means of calculating the time of impact since the collision is considered to be instantaneous. This was the main theory behind the formulation of the linear complementarity problem.

Impact or contact problems are complementary because if bodies are in contact then either there are positive impulses or change in positive relative velocities since both cannot be present at the same time at the same impacting point. This phenomenon yields to a complementary condition in the normal direction to the plane of contact, which can be given as:

$$\Lambda_{Ni}^T > 0, \quad \upsilon_{Ni} > 0 \quad \text{and} \quad \Lambda_{Ni}^T \upsilon_{Ni} = 0 \tag{38}$$

Impact in the normal direction, in the non-smooth frame-work, can be evaluated using two methods leading to the development of the linear complementarity problem. It should be noted that, the definitions of the coefficient of restitution in the two approaches, namely, the Newton's impact law approach and the Poisson's impact law approach, are different.

3.1 Newton's Impact Law

According to the Newton's laws of impact, the coefficient of restitution (ε_N) is the ratio of the post-impact normal relative velocity $\left(\dot{\delta}_N^+\right)$ to the pre-impact normal relative velocity $\left(\dot{\delta}_N^-\right)$ [177]. The pre-impact velocity $\left(\dot{\delta}_N^-\right)$ as per Newton's law of impact, can be given as:

$$\dot{\delta}_N^+ = -\varepsilon_N \dot{\delta}_N^- \tag{39}$$

Now the assumed velocity jump (υ_N) is:

$$\upsilon_N = \dot{\delta}_N^+ + \varepsilon_N \dot{\delta}_N^- \tag{40}$$

Figure 6 depicts the Newton's impact law graphically, where the necessity of the velocity jump (υ_N) is illustrated.

The kinetic equation for impact is:

$$M\left(\dot{\delta}_N^+ - \dot{\delta}_N^-\right) = \Lambda_N \tag{41}$$

where, Λ_N is the impulse.

Thus, a linear complementarity can be derived by combining Eqs. (39), (40) and (41) and can be stated as:

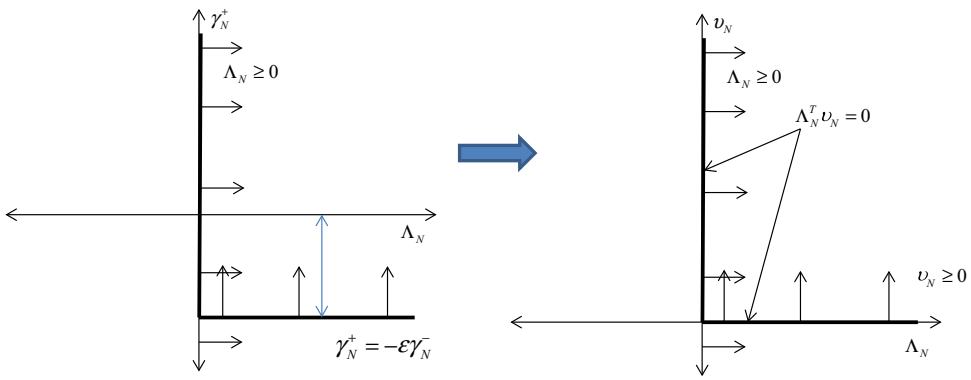

Fig. 6 LCP formulation from Newton's impact law

$$\begin{aligned}\dot{\delta}_N^+ - \dot{\delta}_N^- &= M^{-1}\Lambda_N \\ \dot{\delta}_N^+ &= M^{-1}\Lambda_N + \dot{\delta}_N^- \\ \upsilon_N &= M^{-1}\Lambda_N + (1+\varepsilon_N)\dot{\delta}_N^-\end{aligned} \tag{42}$$

The solution of the linear complementarities shown in Eq. (42) is $\upsilon_N = 0$ because $\dot{\delta}_N^- < 0$, which yields:

$$\begin{aligned}\Lambda_N &= -(1+\varepsilon_N)M\dot{\delta}_N^- \\ \dot{\delta}_N^+ &= -\varepsilon_N\dot{\delta}_N^-\end{aligned} \tag{43}$$

Hence, Eq. (43) gives the relationship of the impulse (Λ_N) and the post-impact velocity $\left(\dot{\delta}_N^+\right)$ with the pre-impact velocity $\left(\dot{\delta}_N^-\right)$.

3.2 Poisson's Impact Law

Poisson described the impact process as a combination of two simultaneous events [100]. At the time of contact, there is a compression followed by an expansion phase, as shown in Fig. 7.

According to Poisson's impact law, the coefficient of restitution is the ratio between the impulse at the compression phase (Λ_{NC}) and to that at the expansion phase (Λ_{NE}). In the case of Poisson's impact, the solution consists of two steps, one for the compression phase and another for the expansion phase. The relationship can be given as:

$$\Lambda_{NE} = \varepsilon_N\Lambda_{NC} \tag{44}$$

Here, the kinetic equation for compression phase of the impact is:

$$M\left(\dot{\delta}_{NC} - \dot{\delta}_N^-\right) = \Lambda_{NC} \tag{45}$$

Thus, a linear complementarity can also be derived by combining Eqs. (39) (40) and (41) and can be written as:

$$\begin{aligned}\dot{\delta}_{NC} - \dot{\delta}_N^- &= M^{-1}\Lambda_{NC} \\ \dot{\delta}_{NC} &= M^{-1}\Lambda_{NC} + \dot{\delta}_N^-\end{aligned} \tag{46}$$

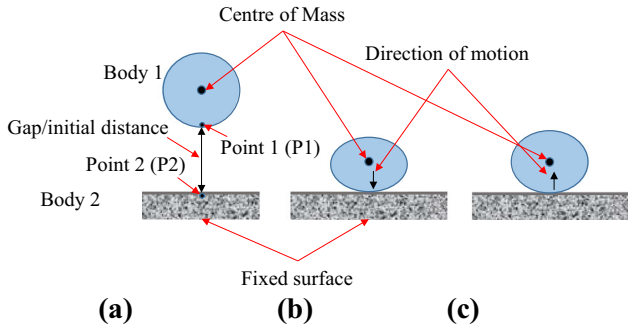

Fig. 7 The impact process according to Poisson's Law illustrating **a** the rest position, **b** the compression stage and **c** the expansion stage

The solution of the linear complementarity of Eq. (46) is $\dot{\delta}_{NC} = 0$ because $\dot{\delta}_N^- < 0$, which yields:

$$\Lambda_{NC} = -M\dot{\delta}_N^- \tag{47}$$

Alternatively, in the expansion phase, ($\Lambda_{NE} > \varepsilon_N\Lambda_{NC}$) and Eq. (47) can only stop the penetration, but for expansion more impulse is required. So, $\Lambda_{NP} = \Lambda_{NE} - \varepsilon_N\Lambda_{NC}$ is assumed in the expansion phase. Here, the kinetic equation for impact becomes:

$$M\left(\dot{\delta}_N^+ - \dot{\delta}_{NC}\right) = \Lambda_{NE} \tag{48}$$

Thus, the linear complementarity for the expansion phase can be derived as:

$$\begin{aligned}\dot{\delta}_N^+ - \gamma_{NC} &= M^{-1}\Lambda_{NC} \\ \dot{\delta}_N^+ &= M^{-1}\Lambda_{NE} + \gamma_{NC} \\ &= M^{-1}\Lambda_{NP} + M^{-1}\varepsilon_N\Lambda_{NC} \\ &= M^{-1}\Lambda_{NP} - \varepsilon_N\dot{\delta}_N^-\end{aligned} \tag{49}$$

The solution of the linear complementarity of Eq. (49) is $\Lambda_{NP} = 0$ because $\gamma_N^- < 0$, which yields:

$$\begin{aligned}\dot{\delta}_N^+ &= -\varepsilon_N\dot{\delta}_N^- \\ \Lambda_{NE} &= \Lambda_{NP} + \varepsilon_N\Lambda_{NC} = -\varepsilon_N M\dot{\delta}_N^-\end{aligned} \tag{50}$$

So, the total impulse throughout the Poisson's impact process is:

$$\Lambda_N = \Lambda_{NC} + \Lambda_{NE} = -M\dot{\delta}_N^- - \varepsilon_N M\dot{\delta}_N^- = -(1+\varepsilon_N)M\dot{\delta}_N^- \tag{51}$$

4 Non-Dimensional Frame

In smooth mechanics, springs are used to simulate the contact behaviour. The relative distance between two bodies (g_N) is defined as $g_N = x - \delta$ where, δ is the gap. In compliances model, impact is not considered as an instantaneous process and it is assumed that contact has very little duration. Since the contact force depends on the contact stiffness, the stiffness increases with the contact force, although the impact duration is shortened. Hence, the impulse $\left(\Lambda = \int_{t_{start}}^{t_{end}} F(t)dt\right)$ is generally independent of the stiffness and the duration. Similarly, for non-smooth models, the main assumption is that the contact happens instantaneously and there is no time lag. Here to compare the different compliances and non-smooth models on the same frame, several dimensionless quantities are proposed.

The contact force ($F(t)$) is mainly dependent on the impacting mass (M) and also on the pre-impact velocity $\left(\dot{\delta}^-\right)$. Since, the contact force is also a function of time, a

new dimensionless quantity, called the dimensionless force, can be introduced as:

$$\tilde{F} = \frac{F(t)\Delta T}{M\dot{\delta}^{-}} = \frac{M\ddot{\delta}\Delta T}{M\dot{\delta}^{-}} = \frac{\ddot{\delta}}{\omega\dot{\delta}^{-}} = \ddot{x} \tag{52}$$

where, $\omega^2 = K/M$, $F(t)$ is the contact force, ΔT represents the duration of the contact and A is the non-dimensional constant. The assumptions considered include, $\delta = Ax$, $t = \tau/\omega$ and $\frac{A\omega}{\dot{\delta}^{-}} = 1$. The time for contact depends entirely on the stiffness and the mass of the impacting bodies. So, dimensionless time can be given as:

$$\tau = \frac{t}{\Delta T} \tag{53}$$

where, Δt is the time difference and is equal to $1/\omega$. Penetration also depends on the mass of impact, pre-impact velocity and stiffness. So, dimensionless penetration can be written as:

$$\tilde{\delta} = \frac{\delta}{\dot{\delta}^{-}\Delta T} = \frac{A\omega x}{\dot{\delta}^{-}} = x \tag{54}$$

Impulse is also dependent on the mass of impact and the pre-impact velocity. Thus, the dimensionless impulse can be represented as:

$$\tilde{\Lambda}_N = \frac{\Lambda_N}{M\dot{\delta}^{-}} = \frac{\int_0^{\Delta T} F(t)dt}{M\dot{\delta}^{-}} \tag{55}$$

where, Λ_N is the dimensional impulse in the normal direction. The impulse can be represented as:

$$\Lambda_N = \frac{\int_0^{\Delta t} F(t)dt}{M\dot{\delta}^{-}} \tag{56}$$

where, Δt is the total time. Now, assuming $\delta = Ax$ and $t = \tau/\omega$, Eq. (55) can be modified to, by incorporating Eqs. (60) and (80), as:

$$\tilde{\Lambda}_N = \frac{\int_0^1 M\ddot{\delta}\frac{d\tau}{\omega}}{M\dot{\delta}^{-}} = \frac{\int_0^1 A\omega^2\ddot{x}\frac{d\tau}{\omega}}{A\omega\dot{x}^{-}} = \frac{\int_0^1 \ddot{x}d\tau}{\dot{x}^{-}} \tag{57}$$

This non-dimensional impulse can be conveniently used for analysing the model.

These dimensionless quantities have been used to converge all the models on the same dimensionless field, so that, they can be effectively and efficiently compared. As it has been elaborately described, there are different kinds of models that have been proposed for different applications. These models have been grouped and sub-grouped into the obvious classes as shown in Fig. 1; hence, the comparison is also carried out for each category individually, in order to make the comparison clear and understandable. The unique and useful models are finally selected and an overall comparison is drawn in between the different class of models.

4.1 Compliance Elastic Model

The equation of motion, for the compliance based elastic models, can be given as:

$$M\ddot{\delta} + K\delta^n = 0 \tag{58}$$

The value of the index n varies for different models and thus a generalised non-dimensional model is given in this part of the review. Equation (58) can again be written as:

$$\ddot{\delta} + \omega^2\delta^n = 0 \tag{59}$$

where, $\omega^2 = K/M$. Now, assuming that $\delta = Ax$ and $t = \tau/\omega$, the acceleration can be derived as:

$$\ddot{\delta} = \frac{d^2\delta}{dt^2} = A\omega^2\frac{d^2x}{d\tau^2} = A\omega^2\ddot{x} \tag{60}$$

Thus, Eq. (58) can be re-written from Eqs. (59) and (60) as:

$$\begin{aligned} &A\omega^2\ddot{x} + \omega^2(Ax)^n = 0 \\ &\Rightarrow \ddot{x} + A^{n-1}x^n = 0 \end{aligned} \tag{61}$$

Now, considering $A^{n-1} = 1$ as the non-dimensional constant, the non-dimensional equation of motion can be written as:

$$\ddot{x} + x^n = 0 \tag{62}$$

Equation (62) is used for comparing the results of all the Hertzian based models.

4.1.1 Contact area Dependent Models

The models, referred in this section, are entirely dependent on the contact area and the material properties of the bodies. Thus, in order to understand the dependency of the impact response, the body is idealised into a sphere. It can be observed from Fig. 2 that the sphere undergoes a virtual penetration of δ and thus the contact area (A) can be calculated as:

$$A = 2\pi\left(2r\delta - \delta^2\right) \tag{63}$$

by using the Pythagoras theorem, where, r is the radius of the sphere. Thus, the force equation can be represented as:

$$F = \frac{4E^*\left(2r\delta^3 - \delta^4\right)^{1/2}}{r} \tag{64}$$

Assuming the same non-dimensional terms, Eq. (64) can be modified to form:

$$F = 4E^*\left(2\frac{A^3x^3}{r} - \frac{A^4x^4}{r^2}\right)^{1/2} \tag{65}$$

Therefore, the non-dimensional equation of motion can be given as:

$$\ddot{x} + \left(x^3 - \alpha x^4\right)^{1/2} = 0 \tag{66}$$

where, $A = 1$ and the other constants are considered as K. K and α are the material and specific geometric dependent parameter. Thus, these models do not have an exact generalised form and are only for particular cases, based on material and or the geometric properties of the contacting bodies, making them incomparable in the present context of generalized models.

4.2 Compliance Energy Dissipating Model

The energy dissipating models under the compliance method, as we have observed, are mainly of two types, Kelvin-element based models and Hertz-damp models. This section illustrates the non-dimensional derivations, used for the comparison of each type.

4.2.1 Kelvin Element Based Model

The equation of motion for the Kelvin element based models can be represented as:

$$M\ddot{\delta} + K\delta + C\dot{\delta} = 0 \tag{67}$$

This model is devoid of any index in the equation of motion and thus the non-dimensional form can be easily derived. Equation (67) can be modified, by dividing both the right-hand and left-hand sides of the equation with M, to form:

$$\ddot{\delta} + \omega^2\delta + 2\xi\omega\dot{\delta} = 0 \tag{68}$$

where, $\omega^2 = K/M$ and $(C/M) = 2\xi\omega$. Again, by assuming the same variables, the non-dimensional velocity can be derived as:

$$\dot{\delta} = \frac{d\delta}{dt} = A\omega\frac{dx}{d\tau} = A\omega\dot{x} \tag{69}$$

The non-dimensional acceleration can be derived similarly, as shown in Eq. (60). Thus, from Eqs. (60), (68) and (69), the equation of motion can be modified as:

$$\begin{aligned} A\omega^2\ddot{x} + \omega^2 Ax + 2\xi\omega^2 A\dot{x} = 0 \\ \Rightarrow \ddot{x} + x + 2\xi\dot{x} = 0 \end{aligned} \tag{70}$$

Thus, the non-dimensional equation of motion is obtained directly from the derivation, without any further assumptions. Thus the equation used for comparing the Kelvin element based models, on the same platform, is:

$$\ddot{x} + x + 2\xi\dot{x} = 0 \tag{71}$$

The value of ξ changes for each model, by modifying which, an effective correlation can be inferred among the available Kelvin-element models.

4.2.2 Hertz-Damp Based Models

The Hertz damp model has been so far the most widely used method for analysing the response of bodies under impact. The various models proposed, originating from this method, can be classified into two types, namely, the pre-impact velocity independent models and the pre-impact velocity dependent models. This section illustrates how the non-dimensional form of the models, of both the types, are derived.

4.2.2.1 Pre-Impact Velocity Independent Models The equation of motion for these types of models can be given as:

$$M\ddot{\delta} + K\delta^n + C\delta^m\dot{\delta} = 0 \tag{72}$$

The values of n and m change with different models and so the generalised non-dimensional equation of motion is derived. Equation (72) can also be modified similarly as:

$$\ddot{\delta} + \omega^2\delta^n + 2\xi\omega\delta^m\dot{\delta} = 0 \tag{73}$$

where, $\omega^2 = K/M$ and $(C/M) = 2\xi\omega$. Considering the same assumptions, Eqs. (60), (69) and (73) can be merged to form the new non-dimensional equation of motion as:

$$A\omega^2\ddot{x} + \omega^2 A^n x^n + 2\xi\omega A^m x^m A\omega\dot{x} = 0 \tag{74}$$

Equation (74) can be further reduced to:

$$\ddot{x} + A^{n-1}x^n + 2\xi A^m x^m\dot{x} = 0 \tag{75}$$

Now, assuming $A^{n-1} = 1$, we can also derive that $A^m = 1 (A \in \Re)$. Thus, Eq. (75) can be rewritten as:

$$\ddot{x} + x^n + 2\xi x^m\dot{x} = 0 \tag{76}$$

which forms the non-dimensional equation of motion. Thus, all the models are made dependent on the value of ξ, which is material dependent and constant, irrespective of the displacements, velocities and accelerations of the concerned bodies. This transformation helps in the proper comparison of the respective types of models, which most of the previous studies have not considered.

4.2.2.2 Pre-Impact Velocity Dependent Models The evolution of the impact models led to the development of many Hertz-damp models that are dependent on the pre-impact velocity. In these models the value of ξ is dependent on the pre-impact velocity of the bodies and on the coefficient of restitution (ε_N). Thus, the value of ξ needs to be non-dimensional in order to provide an effective comparison of the different available models. Therefore, in order to provide a generalised equation of motion, the value of C is taken as:

$$C = Z\frac{K}{\dot{\delta}^{-}} \tag{77}$$

where, Z is either the function of ε_N or of other constants. Therefore, the equation of motion can be given as:

$$\begin{aligned} &M\ddot{\delta} + K\delta^n + C\delta^m\dot{\delta} = 0 \\ &\Rightarrow M\ddot{\delta} + K\delta^n + Z\left(\frac{K}{\dot{\delta}^{-}}\right)\delta^m\dot{\delta} \end{aligned} \tag{78}$$

Equation (78) can be further modified as:

$$\ddot{\delta} + \frac{K}{M}\delta^n + Z\left(\frac{K}{\dot{\delta}^{-}M}\right)\delta^m\dot{\delta} = 0 \tag{79}$$

The pre-impact velocity can be modified, in order to form the non-dimensional pre-impact velocity, assuming $\delta = Ax$ and $t = \tau/\omega$, as:

$$\dot{\delta}^{-} = A\omega\dot{x}^{-} \tag{80}$$

The non-dimensional acceleration and velocity are taken from Eqs. (60) and (69) and also using Eq. (80), the equation of motion can be re-written as:

$$\begin{aligned} &A\omega^2\ddot{x} + \omega A^n x^n + Z\frac{\omega^2}{A\omega\dot{x}^{-}}A^m x^m A\omega\dot{x} = 0 \\ &\Rightarrow \ddot{x} + A^{n-1}x^n + \frac{ZA^m}{\dot{x}^{-}}x^m\dot{x} = 0 \end{aligned} \tag{81}$$

Again, considering $A^{n-1} = 1$, it can be derived that, $A^m = 1$ as $A \in R$ and hence, the equation of motion becomes:

$$\ddot{x} + x^n + \xi x^m = 0 \tag{82}$$

where, $\xi = Z/\dot{x}^{-}$ is dependent only on the constant values of the coefficient of restitution or other coefficients. Thus, by considering Eq. (82), the pre-impact velocity dependent Hertz-damp models can be accurately compared.

5 Comparative Study of the Different Models

Impact models, which represent the models capable of calculating the response of a multi-body system under impact, are generally considered to be ideal when, after experiencing the energy dissipation, the final coefficient of restitution is equal to the initial value previously assumed for solving the governing differential equation of motion. Another important aspect of an ideal model is that the value of the post-impact impulse being analogous to Newton's law [180], which states:

$$\tilde{\Lambda}_N = M\dot{\delta}^{-}(1 + \varepsilon_N) \rightarrow \tilde{\Lambda} = \frac{\Lambda}{M\dot{\delta}^{-}} = 1 + \varepsilon_N \tag{83}$$

This also implies that the area of the hysteresis loop, derived from plotting the force and displacement of the impacting body, which equals the energy lost, should be equal to the value obtained according to Newton's formulation. Considering the mass of the system to be M, the pre-impact velocity to be $\dot{\delta}^{-}$ and the coefficient of restitution to be ε_N in the normal direction, the post-impact (Φ^{+}) and pre-impact (Φ^{-}) kinetic energies can be given as:

$$\begin{aligned} \Phi^{+} &= \frac{1}{2}M\left(\dot{\delta}^{-}\right)^2 \\ \Phi^{-} &= \frac{1}{2}M\varepsilon_N^2\left(\dot{\delta}^{-}\right)^2 \end{aligned} \tag{84}$$

Thus, the energy loss (Ξ) can be calculated as:

$$\begin{aligned} \Xi &= \frac{1}{2}\left(M\left(\dot{\delta}^{-}\right)^2 - M\varepsilon_N^2\left(\dot{\delta}^{-}\right)^2\right) \\ &= \frac{1}{2}M\left(\dot{\delta}^{-}\right)^2\left(1 - \varepsilon_N^2\right) \end{aligned} \tag{85}$$

In the non-dimensional frame, the energy loss becomes:

$$\tilde{\Xi} = \frac{1}{2}\left(1 - \varepsilon_N^2\right) \tag{86}$$

In the present work, in order to carry out an efficient comparison, the coefficient of restitution is maintained at a constant value of 0.5. Thus the area of the hysteresis loop and the equivalent energy loss should be equal to:

$$\tilde{\Xi} = \frac{1}{2}\left(1 - 0.5^2\right) = 0.375 \tag{87}$$

Thus, in the case of an ideal model, the area of the hysteresis loop should be exactly equal to 0.375. In the case of linear spring and Hertz models, the coefficient of restitution plays no part, since there is no energy dissipation. Thus, they are compared separately in this part and though, they form the basis of all the different models, perfect elasticity is only ideal and has little practical applications. Hence, the energy dissipating models have more practicality and provide an improved representation of the real life situation.

5.1 Compliance Elastic Models

The compliance elastic models do not possess any energy dissipating criteria in the equation of motion. Figure 8 illustrates the three different available models which can be categorised into the elastic type. Figure 8a represents the relationship between the dimensionless force and the dimensionless time. It can be observed that the curves are almost similar for all the three cases and thus the non-dimensional impulse is almost two for the cases. These plots were generated with the value of the coefficient of restitution being 0.5 and thus, the actual impulse should be around 1.5. Here lies the first mathematical impracticality of the Hertzian elastic models. Moreover, the comparison

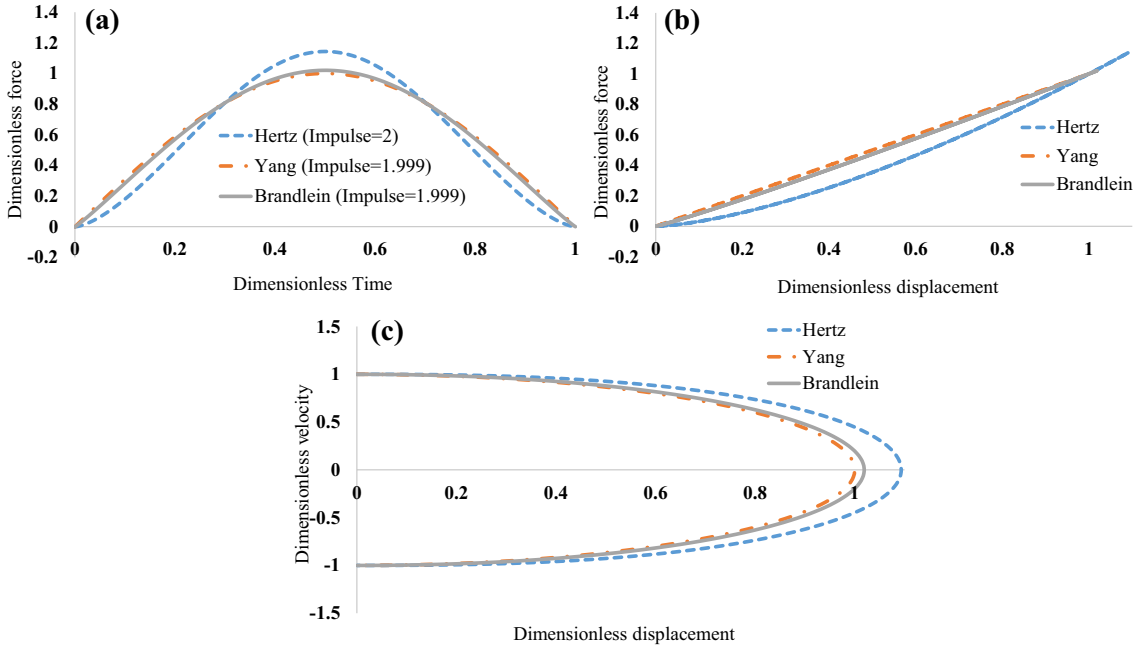

Fig. 8 Comparison among the available, general and unique Hertzian and Linear Spring models with **a** being the force versus time plot, **b** representing the energy loss and **c** is the phase portrait

given in Fig. 8b between the non-dimensional force and the non-dimensional displacement or penetration illustrates the fact that there is no energy loss or dissipation. Thus, these models are theoretical, because the complete absence of energy dissipation is actually impossible in practical. Figure 8c elucidates the final coefficient of restitution attained by the model after the impact phenomenon. The coefficient of restitution for all the models is unity even at the end of the collision phase, thus proving that the models are very well suited to simulate the perfectly elastic collision. Since, there is no dependency on the coefficient of restitution; these models are not practical for modelling the elasto-plastic impact.

5.2 Linear Kelvin Element Based Models

The complexities and the short-comings of the Hertzian elastic model resulted in the evolved contact models by incorporating the Kelvin element into the equation of motion. Three models are available which can be categorised under this section. Figure 9 represents the different responses of the available models in the non-dimensional frame. The variation of the dimensionless force with the dimensionless time shows that all the models experience a high force at the beginning of the contact process, due to the presence of the parallel damper in the Kelvin element. The impulse experienced by the system, according to the model proposed by Anagnostopoulos [20], was observed to be around 1.49, a value which is extremely close to that calculated from Newton's law [180]. The model proposed by Brogliato [100] was also found to predict the non-dimensional impulse response of 1.505, which has even less error when compared to the desired value of impulse. The remaining model was found to have a comparatively higher impulse after the impact phase and thus, lacks practicality. The impractical aspect of the model, proposed by Anagnostopoulos [20], was the possibility of attaining negative force value by the completion of the contact process, as represented in Fig. 9a, b. This problem was not found in either of the models proposed by Goyal et al. [129] and Brogliato [100]. Although, the coefficient of restitution, at the end of the process, was found to be exactly same for Anagnostopoulos's model, a characteristic which was not observed in the cases of the other two models.

A common problem observed in the linear Kelvin element based models was the area of the hysteresis loop and none were found to exactly satisfy Eq. (87); although, two were very close. The variation of the model proposed by Anagnostopoulos [20], when plotted for different coefficients of restitutions, gives a trend as shown in Fig. 10. The general trend in the impulse was found to increase with that of the coefficient of restitution; whereas, the area under the hysteresis loop, i.e., the amount of energy dissipation was observed to decrease. This variation is entirely dependent on the coefficient of restitution, as, with its increase, the model tends to become non-dissipative. Thus, it can be

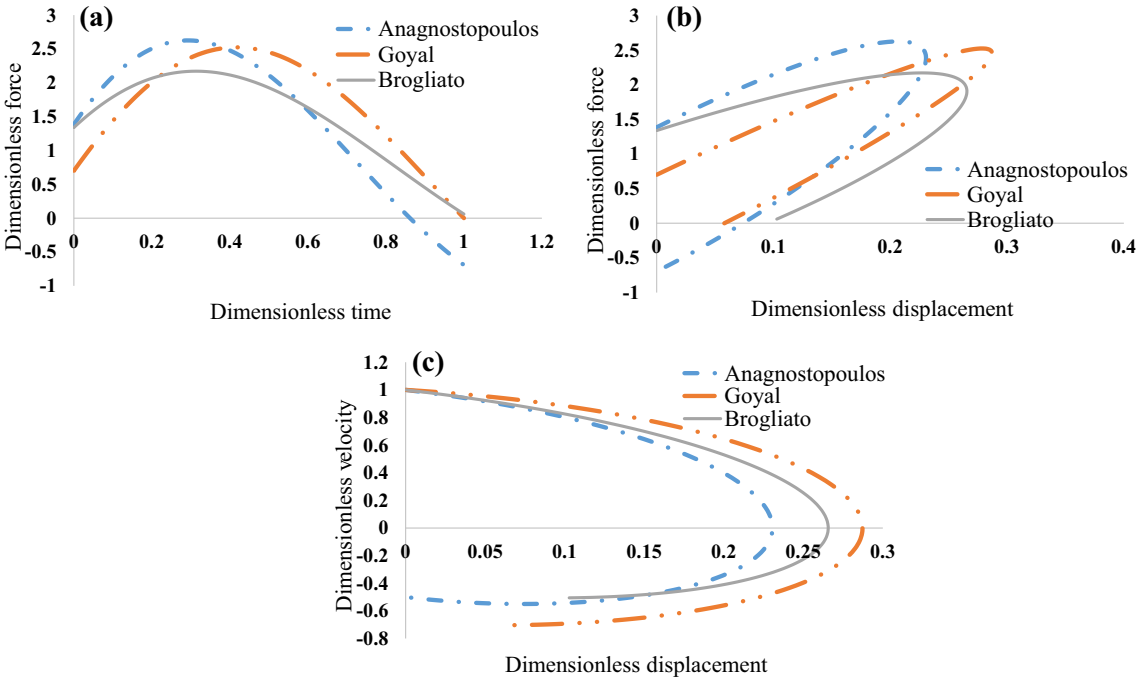

Fig. 9 Comparison among the available, general and unique Kelvin element models with **a** being the force versus time plot, **b** representing the energy loss and **c** is the phase portrait

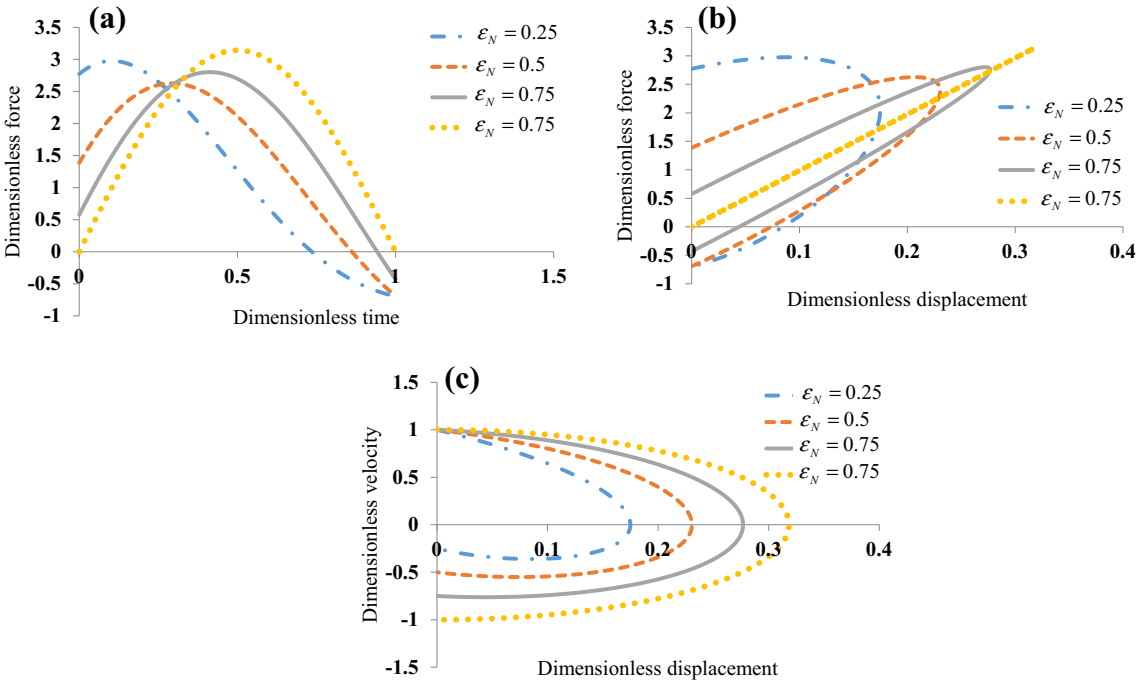

Fig. 10 The variation of the model proposed by Anagnostopoulos [20] when plotted for various coefficients of restitution

inferred, with the value of the coefficient of restitution as unity, the Kelvin model behaves in a way that is analogous to the Hertzian linear model, as can be observed from Figs. 9 and 10.

5.3 Hertz-Damped Models

A further evolution was observed in the contact models, when the damping phenomenon, in the Kelvin element,

was applied to the Hertz law. These models, known as the Hertz-damp models, have seen numerous developments for the last four decades. The main aspect of the development has been the goals of attaining the same coefficient of restitution in the response, as the one considered at the beginning, the value of impulse being analogous to Newton's theory and the area of the hysteresis loop to be exactly equal to that derived in Eq. (87). A comparative analysis among the available Hertz damp models, both continuous and piecewise has been carried out in this section. The models, which are specific geometry and material property dependent, are omitted since; the main aim is to provide a general model which can be used for any geometry and for any material and are solely dependent on the kinetic properties of the system. Moreover, the models addressed are dependent on the general coefficient of restitution of the system, excluding those where the coefficient of restitution and other constants are derived entirely from a particular case, making them non-generic.

Figure 11 illustrates the variation of the non-dimensional force of the general models proposed by different authors for the last few decades. The comparison is plotted for the value of the coefficient of restitution being 0.5 and the best possible response, according to Fig. 11 was observed in the models proposed by Gonthier et al. [138] and Zhiying et al. [153] in the continuous model; whereas, the model proposed by Jankowski [181] being the most ideal model one with regards to the value of impulse. It can also be observed that the maximum error can be found in the model proposed by Herbert et al. [140], with the value of the impulse being extremely low compared to that calculated from Newton's law.

The area formed under the hysteresis loop, by plotting the non-dimensional force with respect to the non-dimensional displacement, represents the amount of energy dissipated during the contact process. Figure 12 represents the comparative study performed on the different Hertz-damp models, in this regard, in order to calculate the amount of energy dissipated and to observe whether they abide by the stereo-mechanical model. The illustration demonstrates that the models proposed by Gonthier [138], Zhiying [153] and Ye [154], although being different in the formulation aspect, provide the same results and almost the same amount of energy dissipation. The maximum amount of energy dissipation was observed in the model proposed by Gharib [156] and the minimum was observed in the model proposed by Lee and Wang [86]. The energy dissipation by all the models is presented in Table 1 and the respective errors are calculated in order to infer the best possible model. Moreover, it can also be observed that all the models follow a smooth trend, except the one proposed by Jankowski, where the response is seen to experience a non-linear rise during the compression phase and an elastic Hertzian response during the expansion phase. The area under the hysteresis loop was found to be 0.373, for the model proposed by Jankowski [181], which can be easily inferred to produce the closest value with regards to the stereo-mechanical model calculated according to Newton's law [180].

Another important aspect for an ideal model is the similarity between the coefficient of restitution used for solving the differential equation initially and the one obtained after the process. Both the values are required to be exactly similar in order to assign a model to be ideal. Figure 13 illustrates the response of the models when the dimensionless velocities are plotted against the dimensionless displacements. Most of the models can be observed to give a coefficient of restitution quite different

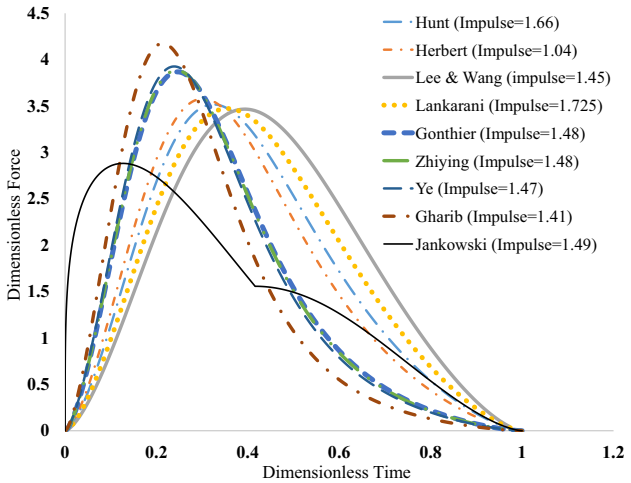

Fig. 11 Comparison between the non-dimensional force and time, of the available general Hertz-damp models when plotted on a unified non-dimensional frame

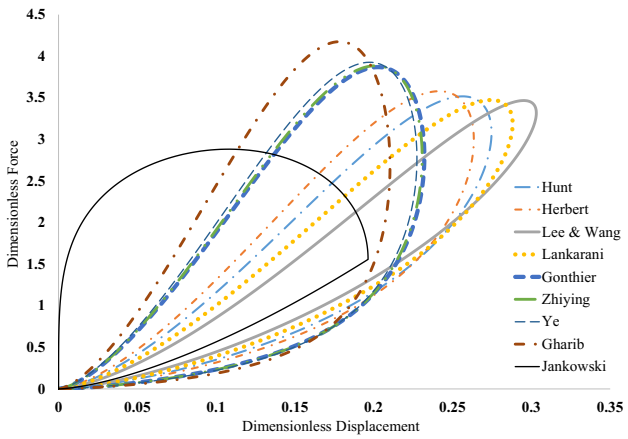

Fig. 12 Comparative study of the non-dimensional force and displacement, among the available general Hertz-damp models when plotted on a unified non-dimensional frame

Table 1 Verification of the compliance models for different coefficients of restitution

References	Error matrix (%)									
	Impulse error (%)				Dissipated energy (%)			Post-impact coefficient of restitution (%)		
Coefficient of restitution	0.25	0.5	0.75	1	0.25	0.5	0.75	0.25	0.5	0.75
Hunt [65]	25.09	10.86	2.81	0.01	27.23	25.31	17.49	125.44	32.60	6.56
Herbert [140]	22.67	7.57	0.13	0.01	23.71	16.88	0.85	113.36	22.70	0.32
Lee and Wang [86]	38.02	19.94	7.92	0.01	49.46	51.87	52.00	190.08	59.84	18.51
Anagnostopoulos [20]	0.01	0.01	0.03	0.03	0.05	0.05	0.07	0.00	0.00	0.00
Lankarani [143]	34.20	15.01	3.99	0.01	42.34	36.83	25.17	171.04	45.04	9.32
Goyal [129]	19.92	13.58	6.18	0.03	6.47	32.83	40.02	50.12	40.84	14.51
Brogliato [100]	0.08	0.41	0.37	0.03	0.01	0.88	1.94	0.48	1.26	0.79
Gonthier [138]	0.42	0.82	1.85	0.01	0.31	1.57	10.77	2.08	2.46	4.29
Jankowski [181]	0.14	0.43	0.85	1.05	0.16	0.51	3.82	3.44	1.08	0.21
Zhiying [153]	3.61	1.16	0.97	0.01	2.63	2.24	5.69	18.04	3.48	2.25
Ye [154]	3.63	1.97	0.81	0.01	2.19	3.79	4.73	18.16	5.92	1.88
Gharib [156]	0.70	5.95	13.19	20.32	0.44	10.80	66.90	3.48	17.86	30.79

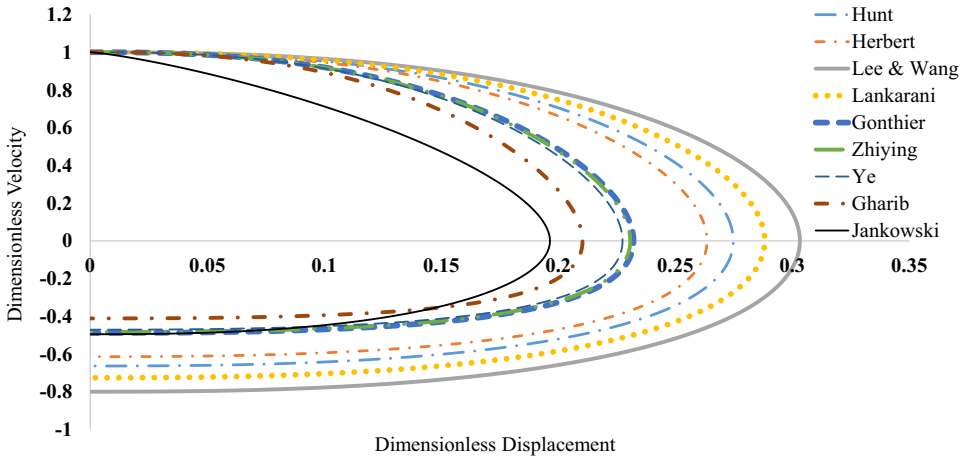

Fig. 13 Comparative study of the non-dimensional velocity and displacement, among the available general Hertz-damp models when plotted on a unified non-dimensional frame

from the input value of 0.5. The models proposed by Zhiying [153], Gonthier [138], Ye [154] and Jankowski [181] were found to yield almost the similar output value of the coefficient of restitution, with the one proposed by Jankowski giving the best result of 0.49. Among all the available continuous compliance models, the ones proposed by Zhiying, Gonthier and Ye were found to have the best response with regard to the ideal nature of any contact model; although, the piecewise method proposed by Jankowski is observed to be more superior to all the continuous Hertz-damp models.

The implicit equations, associated with few of the models, were non-dimensionalised and the value of the damping ratio was thus derived for the constant value of the coefficient of restitution ($\varepsilon_N = 0.5$), for each model. A comprehensive comparison is provided in Table 1 for all the available general models, in order to assess the merits and demerits of each, with regards to the desirable values, according to standard laws.

In order to understand the variation and stability of the superior continuous and piecewise models, the parameters of the models proposed by Ye et al. [154] and Jankowski [181] were varied over four different coefficients of restitution (0.25, 0.5, 0.75 and 1) and the responses are plotted in Figs. 14 and 15 respectively. The model proposed by Ye et al. [154] can be observed to exhibit an extremely stable response for all the coefficients of restitutions, having a similar percentage of error under all the conditions. A linear increase in the value of the post-impact coefficient of restitution and a linear decrease in the amount of energy dissipation was observed with the rise in the value of the coefficient of restitution. Also, the value of the coefficient of restitution in the output was found to be near the desirable value in all the cases, with the amount of

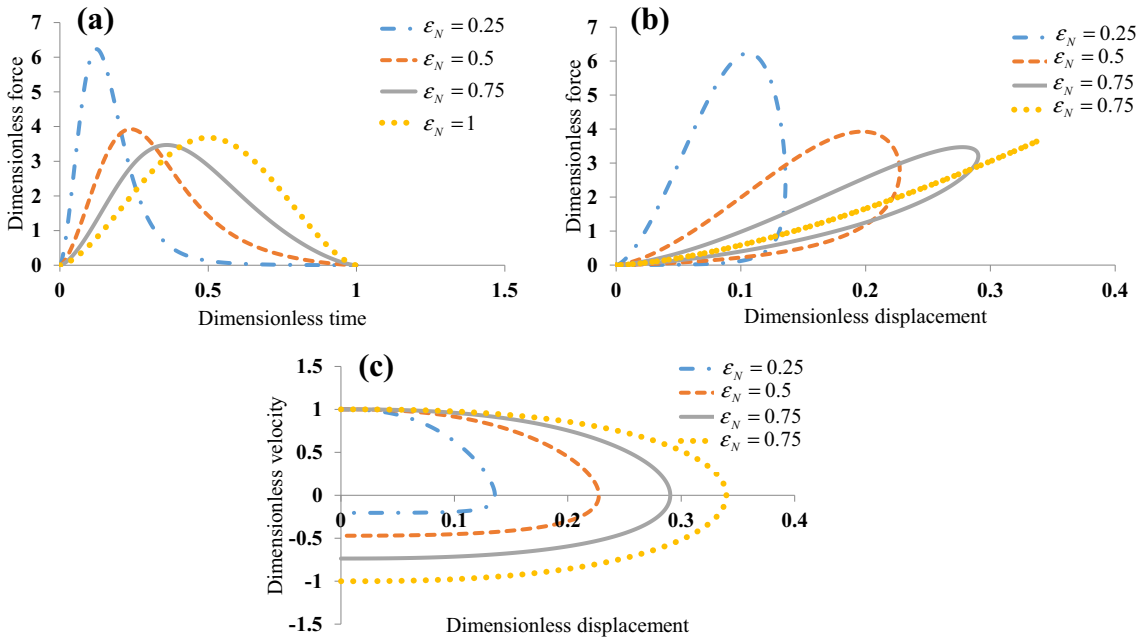

Fig. 14 Variation of the model parameters proposed by Ye et al. [154] when plotted for the various coefficients of restitution

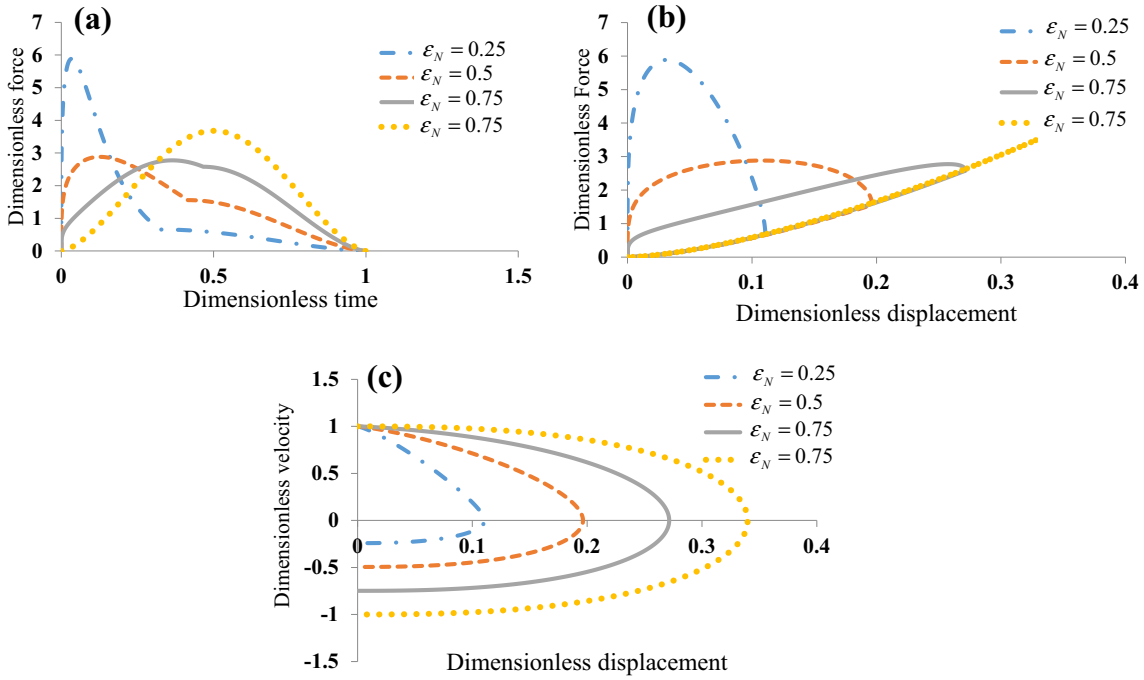

Fig. 15 Variation of the model parameters proposed by Jankowski [181], plotted for the various coefficients of restitution

error increasing to some extent with the decrease in the value of the coefficient of restitution. A similar trend can also be observed in the model proposed by Jankowski [181], only of a much superior nature. The force–time response of the system, though not continuous, is observed to have the best impulse values, and so were the outputs of the hysteresis area and the coefficient of restitution. The model is found to be extremely stable for all the values of ε_N and can be easily inferred to be superior among the rest of the Hertz-damp models.

Thus, it can be inferred, at this point, that the model proposed by Jankowski [181] is the best possible model among all the Hertz-damp models, of both continuous and piecewise types.

5.4 Comparison Among the General Models

A critical comparison is conducted in this section, in order to understand the most appropriate models in the available literature. The response experienced by a particular system, when the different contact models are employed, with respect to the post-impact impulse, the coefficient of restitution and energy dissipation, is simulated on a unified non-dimensional frame. Figure 16 represents the response of the different models. The bars with coloured notations represent the hysteresis area, the variation in the post-impact coefficient of restitution and the impulse respectively. Most of the models are observed to fail in meeting the criterion calculated from the Newton's law and thus, are limited in terms of the practicality and usability. Although, no models were found to replicate the exact response, the models proposed by a few authors can be classified as the most plausible ones.

The errors experienced by all the general models, without any implicit relation, are given in Table 1. The objective of any accurate contact model is its ability to attain the exact coefficient of restitution, as used for solving the force function and for producing the post-impact impulse and the energy dissipation in accordance to the Newton's theory in the stereo-mechanical model. In order to achieve these objectives, the authors have used a forcing function, which is tuned depending on the different coefficients, such as the index values and the damping ratios. In order to validate these modifications, the models should produce the same coefficient of restitution in the post-impact phase, as the one used for solving the differential equation of motion, along with the other two specific parameters. The implicit relations have a specific value of the damping ratios for a specific coefficient of restitution and thus analysing them for a specific value of the coefficient of restitution gives an analogous response when compared to the ones achieved by varying ε_N. It can be observed from Fig. 16 that the available implicit models, namely, the ones proposed by Luo et al. [114] and Zhang et al. [152], do not give the desired response and fail to meet the desired objectives. The model proposed by Tsuji et al. [131] is dependent on the material property and the empirical constant varies according to the different cases. Thus, a variation of the model, for different coefficients of restitution, is beyond the scope of this review. Figure 16 represents the response of the model, for the value of the coefficient of restitution being 0.5, and it can be observed that it gives significant errors.

Table 1 helps in understanding a general trend observed in most of the models, where the percentage of error, in the case of the impulse and the coefficient of restitution, is observed to increase with decreasing coefficient of restitution. A unique and opposite trend in found in the model proposed by Gharib et al. [156], where the percentage of error increases with an increase in the coefficient of restitution. Thus, it can be inferred that most of the models perform poorly when the coefficient of restitution is low; whereas, the one proposed by Gharib gives poor response for higher values of the coefficient of restitution. Three models, as highlighted in Table 1, are found to have extremely small errors, for all the values of the coefficient of restitution. The model proposed by Anagnostopoulos [20] has the best response among all the available compliance models; although, the only disadvantage of the model is the impractical aspect of negative force attained at the end of the expansion phase. The error in the amount of energy dissipation was, in general, found to follow an opposite trend for all the models, with very less stability in all the models.

The most stable models that can be inferred from Table 1 are the ones proposed by Brogliato [100] among

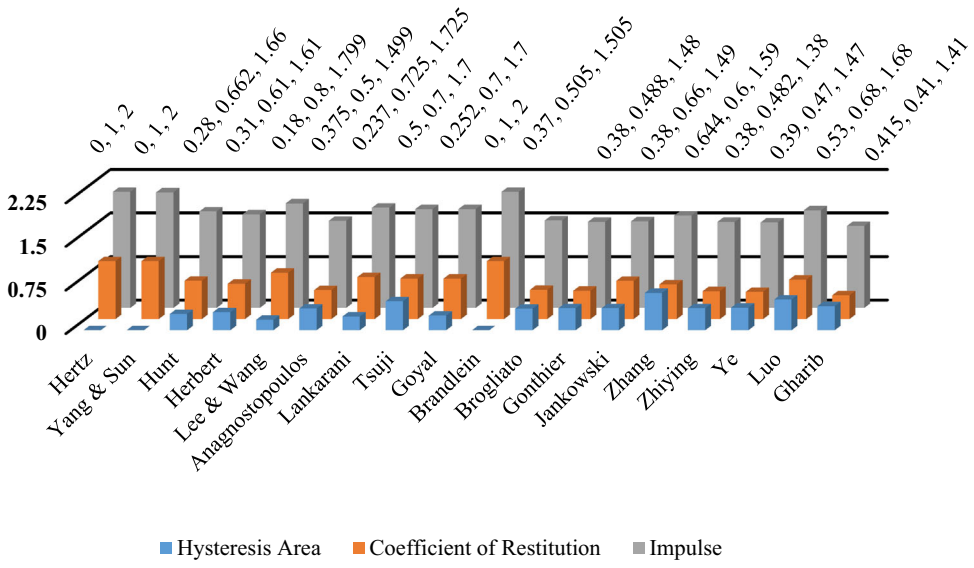

Fig. 16 Comparison of the responses of the available compliance models on the unified non-dimensional frame

all the Kelvin models and Jankowski [181] among all the Hertz-damp models. The variation in the errors, across the different coefficients of restitution, was found to be extremely low when compared to the other models. The model proposed by Brogliato can be observed to be superior to that proposed by Jankowski, for lower values of coefficient of restitution; whereas, for higher values the later model is found to give a better response. Also, the model proposed by Brogliato is observed to have the best stability over all the values, when compared to all the available models.

In spite of all these advantages, the models fail to perform when the coefficient of restitution tends to zero, i.e., for the cases which can be classified as the perfectly plastic collisions. Moreover, the small variation in the most suitable models can also be inferred as inappropriate for precise cases. These problems can be directly eliminated by considering unilateral contacts and it can be observed that the value obtained from Eqs. (43) and (51) are exactly the same as the one obtained from Eq. (83). Hence, the response of the system, by incorporating, unilateral contact, is always exact even for low and high coefficients of restitution.

6 Concluding Remarks

A comprehensive literature survey on the contact modelling techniques is presented in this paper. All the contact models are categorised based on the governing contact laws and finally compared from a unified dimensionless frame to identify the best candidate. Three performance criteria, depending on the post-impact coefficient of restitution, impulse and hysteresis energy output, have been assigned to evaluate their performance. Based on the comparative studies, it can be inferred that the Brogliato's and Jankowski's models are the two best models among all the proposed Kelvin and Hartz-damp formulation respectively; whereas, non-smooth models always yield the desired output. Generally, the errors in compliances models increase with the decrement in the coefficient of restitution and solution of most of the Hertzian model becomes unstable for the purely plastic collision. However, the non-smooth models and Kelvin elements are stable in all ranges of coefficients of restitution.

References

1. Flores P et al (2008) Kinematics and dynamics of multibody systems with imperfect joints: models and case studies, vol 34. Springer, Berlin
2. Nikravesh PE (2008) Newtonian-based methodologies in multibody dynamics. Proc Inst Mech Eng Part K J Multi-body Dyn 222(4):277–288
3. Nikravesh PE (1988) Computer-aided analysis of mechanical systems. Prentice-Hall, Inc, Upper Saddle River
4. Ambrósio J, Verissimo P (2009) Improved bushing models for general multibody systems and vehicle dynamics. Multibody Syst Dyn 22(4):341–365
5. Flores P (2009) Modeling and simulation of wear in revolute clearance joints in multibody systems. Mech Mach Theory 44(6):1211–1222
6. Machado M et al (2010) Development of a planar multibody model of the human knee joint. Nonlinear Dyn 60(3):459–478
7. Alves J et al (2015) A comparative study of the viscoelastic constitutive models for frictionless contact interfaces in solids. Mech Mach Theory 85:172–188
8. Bhalerao K, Anderson K (2010) Modeling intermittent contact for flexible multibody systems. Nonlinear Dyn 60(1–2):63–79
9. Choi J et al (2010) An efficient and robust contact algorithm for a compliant contact force model between bodies of complex geometry. Multibody Syst Dyn 23(1):99–120
10. Ebrahimi S, Hippmann G, Eberhard P (2005) Extension of the polygonal contact model for flexible multibody systems. Int J Appl Math and Mech 1(1):33–50
11. Flores P, Leine R, Glocker C (2012) Application of the nonsmooth dynamics approach to model and analysis of the contact-impact events in cam-follower systems. Nonlinear Dyn 69(4):2117–2133
12. Hirschkorn M, McPhee J, Birkett S (2005) Dynamic modeling and experimental testing of a piano action mechanism. J Comput Nonlinear Dyn 1(1):47–55
13. Minamoto H, Kawamura S (2011) Moderately high speed impact of two identical spheres. Int J Impact Eng 38(2–3):123–129
14. Dimitrakopoulos E (2010) Analysis of a frictional oblique impact observed in skew bridges. Nonlinear Dyn 60(4):575–595
15. Dimitrakopoulos E, Kappos AJ, Makris N (2009) Dimensional analysis of yielding and pounding structures for records without distinct pulses. Soil Dyn Earthq Eng 29(7):1170–1180
16. Dimitrakopoulos E, Makris N, Kappos A (2010) dimensional analysis of the earthquake response of a pounding oscillator. J Eng Mech 136(3):299–310
17. Dimitrakopoulos E, Makris N, Kappos AJ (2009) Dimensional analysis of the earthquake-induced pounding between adjacent structures. Earthq Eng Struct Dyn 38(7):867–886
18. Dimitrakopoulos EG (2013) Nonsmooth analysis of the impact between successive skew bridge-segments. Nonlinear Dyn 74(4):911–928
19. Julian FDR, Hayashikawa T, Obata T (2007) Seismic performance of isolated curved steel viaducts equipped with deck unseating prevention cable restrainers. J Constr Steel Res 63(2):237–253
20. Anagnostopoulos SA (1988) Pounding of buildings in series during earthquakes. Earthq Eng Struct Dyn 16(3):443–456
21. Anagnostopoulos SA, Spiliopoulos KV (1992) An investigation of earthquake induced pounding between adjacent buildings. Earthq Eng Struct Dyn 21(4):289–302
22. Cole G et al (2010) Interbuilding pounding damage observed in the 2010 Darfield earthquake. Bull N Z Soc Earthq Eng 43(4):382
23. Cole GL (2012) The effects of detailed analysis on the prediction of seismic building ounding performance in Civil Engineering. University of Canterbury, Canterbury
24. Cole GL, Dhakal RP, Turner FM (2012) Building pounding damage observed in the 2011 Christchurch earthquake. Earthq Eng Struct Dyn 41(5):893–913
25. Fleischmann J (2015) DEM-PM contact model with multi-step tangential contact displacement history. Simulation-Based Engineering Laboratory, University of Wisconsin-Madison, Madison

26. Mishra BK (2003) A review of computer simulation of tumbling mills by the discrete element method: part II—practical applications. Int J Miner Process 71(1–4):95–112
27. Williams JR, O'Connor R (1999) Discrete element simulation and the contact problem. Arch Comput Methods Eng 6(4): 279–304
28. Beheshti HK, Lankarani HM (2006) A simplified test methodology for crashworthiness evaluation of aircraft seat cushions. Int J Crashworthiness 11(1):27–35
29. Carvalho M, Ambrosio J (2011) Development of generic road vehicle multibody models for crash analysis using an optimisation approach. Int J Crashworthiness 16(5):537–556
30. Sousa L, Veríssimo P, Ambrósio J (2008) Development of generic multibody road vehicle models for crashworthiness. Multibody Syst Dyn 19(1–2):133–158
31. Erkaya S, Uzmay İ (2008) A neural–genetic (NN–GA) approach for optimising mechanisms having joints with clearance. Multibody Syst Dyn 20(1):69–83
32. Flores P, Lankarani H (2010) Spatial rigid-multibody systems with lubricated spherical clearance joints: modeling and simulation. Nonlinear Dyn 60(1–2):99–114
33. Xu L-X et al (2012) Modeling and analysis of planar multibody systems containing deep groove ball bearing with clearance. Mech Mach Theory 56:69–88
34. Izadbakhsh A, McPhee J, Birkett S (2008) Dynamic modeling and experimental testing of a piano action mechanism with a flexible hammer shank. J Comput Nonlinear Dyn 3(3):031004
35. Hegazy S, Rahnejat H, Hussain K (2000) Multi-body dynamics in full-vehicle handling analysis under transient manoeuvre. Veh Syst Dyn 34(1):1–24
36. Iwnicki S (2006) Handbook of railway vehicle dynamics. CRC Press, Boca Raton
37. Jalili MM, Salehi H (2011) Wheel/rail contact model for rail vehicle dynamics. C R Mécanique 339(11):700–707
38. Mermertas V (1998) Dynamic interaction between the vehicle and simply supported curved bridge deck. Comput Methods Appl Mech Eng 162(1):125–131
39. Rubinstein D, Hitron R (2004) A detailed multi-body model for dynamic simulation of off-road tracked vehicles. J Terrramech 41(2–3):163–173
40. Shabana A, Sany J (2001) A survey of rail vehicle track simulations and flexible multibody dynamics. Nonlinear Dyn 26(2): 179–212
41. Vollebregt E, Segal G (2014) Solving conformal wheel–rail rolling contact problems. Vehicle System Dynamics 52(sup1): 455–468
42. Weidemann C (2010) State-of-the-art railway vehicle design with multi-body simulation. J Mech Syst Transp Logist 3(1): 12–26
43. Yang YB, Yau J (1997) Vehicle-bridge interaction element for dynamic analysis. J Struct Eng 123(11):1512–1518
44. Yang YB, Lin CW (2005) Vehicle–bridge interaction dynamics and potential applications. J Sound Vib 284(1–2):205–226
45. Bi SS, Zhou XD, Marghitu DB (2012) Impact modelling and analysis of the compliant legged robots. Proc Inst Mech Eng Part K J Multi-body Dyn 226(2):85–94
46. Marhefka DW, Orin DE (1999) A compliant contact model with nonlinear damping for simulation of robotic systems. IEEE Trans Syst Man Cybern Part A Syst Hum 29(6):566–572
47. Verscheure D et al (2010) Identification of contact parameters from stiff multi-point contact robotic operations. Int J Robot Res 29(4):367–385
48. Argatov I (2012) Development of an asymptotic modeling methodology for tibio-femoral contact in multibody dynamic simulations of the human knee joint. Multibody Syst Dyn 28(1–2):3–20
49. Argatov I, Mishuris G (2015) Articular contact mechanics. In: Contact mechanics of articular cartilage layers. Springer: Berlin, pp 229–259
50. Askari E et al (2014) Study of the friction-induced vibration and contact mechanics of artificial hip joints. Tribol Int 70:1–10
51. Morales-Orcajo E, Bayod J, Barbosa de Las Casas E (2015) Computational foot modeling: scope and applications. Arch Comput Methods Eng. doi:10.1007/s11831-015-9146-z
52. Silva P, Silva M, Martins J (2010) Evaluation of the contact forces developed in the lower limb/orthosis interface for comfort design. Multibody Syst Dyn 24(3):367–388
53. Das R, Cleary PW (2010) Effect of rock shapes on brittle fracture using Smoothed Particle Hydrodynamics. Theor Appl Fract Mech 53(1):47–60
54. Das R, Cleary PW (2008) Modelling 3D fracture and fragmentation in a thin plate under high velocity projectile impact using SPH. In: 3rd SPHERIC workshop. Lausanne, Switzerland
55. Liu M, Liu G (2010) Smoothed particle hydrodynamics (SPH): an overview and recent developments. Arch Comput Methods Eng 17(1):25–76
56. Das R, Cleary PW (2008) Modelling brittle fracture and fragmentation of a column during projectile impact using a meshfree method. In: 6th International Conference on CFD in Oil & Gas, Metallurgical and Process Industries. Trondheim, Norway
57. Das R, Rao S, Lin RJT (2013) Impact behaviour of elastomer based fibre metal laminates. In: Proceedings of the 19th International Conference on Composite Materials (ICCM19). Montreal, Canada
58. Shaw MC, Das R, Chanda A (2016) 3.11 damage tolerance, reliability and fracture characteristics of multilayered engineering composites. In: Reference Module in Materials Science and Materials Engineering. Elsevier: New York
59. Dopico D et al (2011) Dealing with multiple contacts in a human-in-the-loop application. Multibody Syst Dyn 25(2): 167–183
60. Gonzalez-Perez I, Iserte JL, Fuentes A (2011) Implementation of Hertz theory and validation of a finite element model for stress analysis of gear drives with localized bearing contact. Mech Mach Theory 46(6):765–783
61. Pham H-T, Wang D-A (2011) A constant-force bistable mechanism for force regulation and overload protection. Mech Mach Theory 46(7):899–909
62. Zhu S, Zwiebel S, Bernhardt G (1999) A theoretical formula for calculating damping in the impact of two bodies in a multibody system. Proc Inst Mech Eng Part C J Mech Eng Sci 213(3): 211–216
63. Machado M et al (2012) Compliant contact force models in multibody dynamics: evolution of the Hertz contact theory. Mech Mach Theory 53:99–121
64. Dietl P, Wensing J, Van Nijen G (2000) Rolling bearing damping for dynamic analysis of multi-body systems—experimental and theoretical results. Proc Inst Mech Eng Part K J Multi-body Dyn 214(1):33–43
65. Hunt KH, Crossley FRE (1975) Coefficient of restitution interpreted as damping in vibroimpact. J Appl Mech 42(2):440–445
66. Moreira P, Flores , Silva M (2012) A biomechanical multibody foot model for forward dynamic analysis. In: Bioengineering (ENBENG), 2012 IEEE 2nd Portuguese Meeting, IEEE
67. Hertz H (1882) Über die Berührung fester elastischer Körper. Journal für die Reine und Angewandte Mathematik 29:156–171
68. Hertz H (1881) On the contact of elastic solids. J Reine Angew Math 92(156–171):110
69. Inc A (2007) ANSYS Theory Manual, Release 11
70. ABAQUS U (2001) User's and Theory Manuals. HKS Inc.: Pawtuchet, US
71. Manual AUS (2007) Version 6.7. Hibbit, Karlsson & Sorensen

72. Wriggers P, Laursen TA (2006) Computational contact mechanics, vol 30167. Springer, Berlin
73. Flores P et al (2007) Dynamic behaviour of planar rigid multibody systems including revolute joints with clearance. Proc Inst Mech Eng Part K J Multi-body Dyn 221(2):161–174
74. Pereira MS, Nikravesh P (1996) Impact dynamics of multibody systems with frictional contact using joint coordinates and canonical equations of motion. Nonlinear Dyn 9(1–2):53–71
75. Mahmoud S, Jankowski R (2011) Modified linear viscoelastic model of earthquake-induced structural pounding. Iran J Sci Technol 35:51–62
76. Shivaswamy S, Lankarani HM (1997) Impact analysis of plates using quasi-static approach. J Mech Des 119(3):376–381
77. Flores P, Ambrósio J (2010) On the contact detection for contact-impact analysis in multibody systems. Multibody Syst Dyn 24(1):103–122
78. Greenwood DT (1988) Principles of dynamics. Prentice-Hall, Englewood Cliffs
79. Lankarani H, Nikravesh P (1988) Application of the canonical equations of motion in problems of constrained multibody systems with intermittent motion. Adv Des Autom 1:417–423
80. Shabana AA (2013) Dynamics of multibody systems. Cambridge University Press, Cambridge
81. van Mier JG et al (1991) Load-time response of colliding concrete bodies. J Struct Eng 117(2):354–374
82. Goldsmith W (2001) Impact. Courier Corporation, North Chelmsford
83. Stronge WJ (2004) Impact mechanics. Cambridge University Press, Cambridge
84. Zhang X, Vu-Quoc L (2002) Modeling the dependence of the coefficient of restitution on the impact velocity in elasto-plastic collisions. Int J Impact Eng 27(3):317–341
85. Jackson RL, Green I, Marghitu DB (2010) Predicting the coefficient of restitution of impacting elastic-perfectly plastic spheres. Nonlinear Dyn 60(3):217–229
86. Lee TW, Wang AC (1983) On the dynamics of intermittent-motion mechanisms. Part 1: dynamic model and response. J Mech Transm Autom Des 105(3):534–540
87. Najafabadi SAM, Kövecses J, Angeles J (2008) Generalization of the energetic coefficient of restitution for contacts in multibody systems. J Comput Nonlinear Dyn 3(4):041008
88. Seifried R, Schiehlen W, Eberhard P (2010) The role of the coefficient of restitution on impact problems in multi-body dynamics. Proc Inst Mech Eng Part K J Multi-body Dyn 224(3):279–306
89. Zhang Y, Sharf I (2009) Validation of nonlinear viscoelastic contact force models for low speed impact. J Appl Mech 76(5):051002
90. Glocker C (2001) On frictionless impact models in rigid-body systems. Philos Trans R Soc Lond A Math Phys Eng Sci 359(1789):2385–2404
91. Glocker C (2001) Set-valued force laws: dynamics of non-smooth systems, vol 1. Springer, Berlin
92. Atkinson KE (2008) An introduction to numerical analysis. Wiley, New York
93. Gilardi G, Sharf I (2002) Literature survey of contact dynamics modelling. Mech Mach Theory 37(10):1213–1239
94. Glocker C (2004) Concepts for modeling impacts without friction. Acta Mech 168(1–2):1–19
95. Hippmann G (2004) An algorithm for compliant contact between complexly shaped bodies. Multibody Syst Dyn 12(4):345–362
96. Lopes DS et al (2010) A mathematical framework for rigid contact detection between quadric and superquadric surfaces. Multibody Syst Dyn 24(3):255–280
97. Flores P, Ambrósio J (2004) Revolute joints with clearance in multibody systems. Comput Struct 82(17–19):1359–1369
98. Flores P, Leine R, Glocker C (2011) Modeling and analysis of rigid multibody systems with translational clearance joints based on the nonsmooth dynamics approach. In: Arczewski K et al (eds) Multibody dynamics. Springer, Netherlands, pp 107–130
99. Johnson K (1982) One hundred years of Hertz contact. Proc Inst Mech Eng 196(1):363–378
100. Brogliato B (1999) Nonsmooth mechanics: models, dynamics and control. Springer, Berlin
101. Guess TM, Maletsky LP (2005) Computational modelling of a total knee prosthetic loaded in a dynamic knee simulator. Med Eng Phys 27(5):357–367
102. Yang D, Sun Z (1985) A rotary model for spur gear dynamics. J Mech Des 107(4):529–535
103. Dubowsky S, Freudenstein F (1971) Dynamic analysis of mechanical systems with clearances—part 1: formation of dynamic model. J Eng Ind 93(1):305–309
104. Cundall PA, Strack OD (1979) A discrete numerical model for granular assemblies. Geotechnique 29(1):47–65
105. Flores P et al (2008) Translational joints with clearance in rigid multibody systems. J Comput Nonlinear Dyn 3(1):011007
106. Pereira CM, Ramalho AL, Ambrósio JA (2011) A critical overview of internal and external cylinder contact force models. Nonlinear Dyn 63(4):681–697
107. Brändlein J (1995) Die Wälzlagerpraxis. Handbuch für die Berechnung und Gestaltung von Lagerungen. Mainz: Vereinigte Fachverlage,| c1995, 3., neu bearb. Aufl., edited by Braendlein, Johannes, 1
108. Van Nijen G (2001) On the overrolling of local imperfection in rolling bearings. Ph.D. Thesis, University of Twente, Enschede, the Netherlands
109. Johnson KL, Johnson KL (1987) Contact mechanics. Cambridge University Press, Cambridge
110. Goodman L, Keer L (1965) The contact stress problem for an elastic sphere indenting an elastic cavity. Int J Solids Struct 1(4):407–415
111. Liu C, Zhang K, Yang L (2005) The compliance contact model of cylindrical joints with clearances. Acta Mech Sin 21(5):451–458
112. Tian Q et al (2011) A new model for dry and lubricated cylindrical joints with clearance in spatial flexible multibody systems. Nonlinear Dyn 64(1–2):25–47
113. Liu C-S, Zhang K, Yang L (2005) Normal force-displacement relationship of spherical joints with clearances. J Comput Nonlinear Dyn 1(2):160–167
114. Luo L, Nahon M (2005) A compliant contact model including interference geometry for polyhedral objects. J Comput Nonlinear Dyn 1(2):150–159
115. Luo L, Nahon M (2010) Development and validation of geometry-based compliant contact models. J Comput Nonlinear Dyn 6(1):011004
116. Bei Y, Fregly BJ (2004) Multibody dynamic simulation of knee contact mechanics. Med Eng Phys 26(9):777–789
117. Pérez-González A et al (2008) A modified elastic foundation contact model for application in 3D models of the prosthetic knee. Med Eng Phys 30(3):387–398
118. Mukras SM et al. (2010) Evaluation of contact force and elastic foundation models for wear analysis of multibody systems. In: ASME 2010 International Design Engineering Technical Conferences and Computers and Information in Engineering Conference. American Society of Mechanical Engineers
119. Dubowsky S, Deck J, Costello H (1987) The dynamic modeling of flexible spatial machine systems with clearance connections. J Mech Des 109(1):87–94
120. Dubowsky S, Freudenstein F (1971) Dynamic analysis of mechanical systems with clearances—part 2: dynamic response. J Manuf Sci Eng 93(1):310–316

121. Dubowsky S, Gardner T (1977) Design and analysis of multilink flexible mechanisms with multiple clearance connections. J Manuf Sci Eng 99(1):88–96
122. Dubowsky S, Young S (1975) An experimental and analytical study of connection forces in high-speed mechanisms. J Manuf Sci Eng 97(4):1166–1174
123. Rogers R, Andrews G (1977) Dynamic simulation of planar mechanical systems with lubricated bearing clearances using vector-network methods. J Manuf Sci Eng 99(1):131–137
124. Khulief Y, Shabana A (1987) A continuous force model for the impact analysis of flexible multibody systems. Mech Mach Theory 22(3):213–224
125. Fox B, Jennings L, Zomaya A (2001) Numerical computation of differential-algebraic equations for non-linear dynamics of multibody systems involving contact forces. J Mech Des 123(2):272–281
126. Hegazy S, Rahnejat H, Hussain K (1999) Multi-body dynamics in full-vehicle handling analysis. Proc Inst Mech Eng Part K J Multi-body Dyn 213(1):19–31
127. Bibalan PT, Featherstone R (2009) A study of soft contact models in simulink. In: Australasian Conference on Robotics and Automation. Citeseer
128. Goyal S, Pinson E, Sinden F (1994) Simulation of dynamics of interacting rigid bodies including friction I: general problem and contact model. Eng Comput 10(3):162–174
129. Goyal S, Pinson EN, Sinden FW (1994) Simulation of dynamics of interacting rigid bodies including friction II: software system design and implementation. Eng Comput 10(3):175–195
130. Kuwabara G, Kono K (1987) Restitution coefficient in a collision between two spheres. Jpn J Appl Phys 26(8R):1230
131. Tsuji Y, Tanaka T, Ishida T (1992) Lagrangian numerical simulation of plug flow of cohesionless particles in a horizontal pipe. Powder Technol 71(3):239–250
132. Lee J, Herrmann HJ (1993) Angle of repose and angle of marginal stability: molecular dynamics of granular particles. J Phys A: Math Gen 26(2):373
133. Brilliantov NV et al (1996) Model for collisions in granular gases. Phys Rev E 53(5):5382–5392
134. Brilliantov NV et al (1996) The collision of particles in granular systems. Phys A 231(4):417–424
135. Schwager T, Pöschel T (1998) Coefficient of normal restitution of viscous particles and cooling rate of granular gases. Phys Rev E 57(1):650–654
136. Bordbar M, Hyppänen T (2007) Modeling of binary collision between multisize viscoelastic spheres. J Numer Anal Ind Appl Math 2(3–4):115–128
137. Guess TM et al (2010) A subject specific multibody model of the knee with menisci. Med Eng Phys 32(5):505–515
138. Gonthier Y et al (2004) A regularized contact model with asymmetric damping and dwell-time dependent friction. Multibody Syst Dyn 11(3):209–233
139. Papetti S, Avanzini F, Rocchesso D (2011) Numerical methods for a nonlinear impact model: a comparative study with closed-form corrections. IEEE Trans Audio Speech Lang Process 19(7):2146–2158
140. Herbert RG, McWhannell DC (1977) Shape and frequency composition of pulses from an impact pair. J Eng Ind 99(3):513–518
141. Sarkar N, Ellis RE, Moore TN (1997) Backlash detection in geared mechanisms: modeling, simulation, and experimentation. Mech Syst Signal Process 11(3):391–408
142. Yigit AS, Ulsoy AG, Scott RA (1990) Spring-dashpot models for the dynamics of a radially rotating beam with impact. J Sound Vib 142(3):515–525
143. Lankarani HM, Nikravesh PE (1990) A contact force model with hysteresis damping for impact analysis of multibody systems. J Mech Des 112(3):369–376
144. Shivaswamy S (1997) Modeling contact forces and energy dissipation during impact in mechanical systems. Wichita State University, Departemnt of Mechanical Engineering, Wichita
145. Ivanov AP (1996) Bifurcations in impact systems. Chaos, Solitons Fractals 7(10):1615–1634
146. Lee H-S, Yoon Y-S (1994) Impact analysis of flexible mechanical system using load-dependent Ritz vectors. Finite Elem Anal Des 15(3):201–217
147. Pereira CM, Ambrósio JA, Ramalho AL (2010) A methodology for the generation of planar models for multibody chain drives. Multibody Syst Dyn 24(3):303–324
148. Schwab A, Meijaard J, Meijers P (2002) A comparison of revolute joint clearance models in the dynamic analysis of rigid and elastic mechanical systems. Mech Mach Theory 37(9):895–913
149. Wasfy TM, Noor AK (2003) Computational strategies for flexible multibody systems. Appl Mech Rev 56(6):553–613
150. Muthukumar S, DesRoches R (2006) A Hertz contact model with non-linear damping for pounding simulation. Earthq Eng Struct Dyn 35(7):811–828
151. Lankarani HM, Nikravesh PE (1994) Continuous contact force models for impact analysis in multibody systems. Nonlinear Dyn 5(2):193–207
152. Zhang Y, Sharf I (2004) Compliant force modelling for impact analysis. In: ASME 2004 International Design Engineering Technical Conferences and Computers and Information in Engineering Conference. American Society of Mechanical Engineers
153. Zhiying Q, Qishao L (2006) Analysis of impact process based on restitution coefficient. J Dyn Control 4:294–298
154. Ye K, Li L, Zhu H (2009) A note on the Hertz contact model with nonlinear damping for pounding simulation. Earthq Eng Struct Dyn 38(9):1135–1142
155. Flores P et al (2011) On the continuous contact force models for soft materials in multibody dynamics. Multibody Syst Dyn 25(3):357–375
156. Gharib M, Hurmuzlu Y (2012) A new contact force model for low coefficient of restitution impact. J Appl Mech 79(6):064506
157. Khatiwada S, Chouw N, Butterworth JW (2014) A generic structural pounding model using numerically exact displacement proportional damping. Eng Struct 62–63:33–41
158. Burgin LV, Aspden RM (2008) Impact testing to determine the mechanical properties of articular cartilage in isolation and on bone. J Mater Sci Mater Med 19(2):703–711
159. Falcon E et al (1998) Behavior of one inelastic ball bouncing repeatedly off the ground. Eur Phys J B Condens Matter Complex Syst 3(1):45–57
160. Gugan D (2000) Inelastic collision and the Hertz theory of impact. Am J Phys 68(10):920–924
161. Kagami J, Yamada K, Hatazawa T (1983) Contact between a sphere and rough plates. Wear 87(1):93–105
162. Minamoto H, Kawamura S (2009) Effects of material strain rate sensitivity in low speed impact between two identical spheres. Int J Impact Eng 36(5):680–686
163. Půst L, Peterka F (2003) Impact oscillator with Hertz's model of contact. Meccanica 38(1):99–116
164. Ramírez R et al (1999) Coefficient of restitution of colliding viscoelastic spheres. Phys Rev E 60(4):4465
165. Rigaud E, Perret-Liaudet J (2003) Experiments and numerical results on non-linear vibrations of an impacting Hertzian contact. Part 1: harmonic excitation. J Sound Vib 265(2):289–307
166. Tatara Y (1989) Extensive theory of force-approach relations of elastic spheres in compression and in impact. J Eng Mater Technol 111(2):163–168
167. Tatara Y, Moriwaki N (1982) Study on impact of equivalent two bodies: coefficients of restitution of spheres of brass, lead, glass,

porcelain and agate, and the material properties. Bull JSME 25(202):631–637
168. Villaggio P (1996) The rebound of an elastic sphere against a rigid wall. J Appl Mech 63(2):259–263
169. Vu-Quoc L, Zhang X, Lesburg L (2001) Normal and tangential force–displacement relations for frictional elasto-plastic contact of spheres. Int J Solids Struct 38(36):6455–6489
170. Vu-Quoc L, Zhang X, Lesburg L (1999) A normal force-displacement model for contacting spheres accounting for plastic deformation: force-driven formulation. J Appl Mech 67(2): 363–371
171. Wu C-Y, Li L-Y, Thornton C (2005) Energy dissipation during normal impact of elastic and elastic–plastic spheres. Int J Impact Eng 32(1):593–604
172. Wu C-Y, Li L-Y, Thornton C (2003) Rebound behaviour of spheres for plastic impacts. Int J Impact Eng 28(9):929–946
173. Yoshioka N (1997) A review of the micromechanical approach to the physics of contacting surfaces. Tectonophysics 277(1): 29–40
174. Zhang X, Lesburg L (2000) A normal force-displacement model for contacting spheres accounting for plastic deformation: force-driven formulation. J Appl Mech 67:363–371
175. Valles RE, Reinhorn AM (1997) Evaluation, prevention and mitigation of pounding effects in building structures. National Center for Earthquake Engineering Research, University of Buffalo, Buffalo
176. Valles-Mattox R, Reinhorn A (1996) Evaluation, prevention and mitigation of pounding effects in building structures. In: Eleventh World Conference on Earthquake Engineering
177. Pfeiffer F, Glocker C (2000) Multibody dynamics with unilateral contacts, vol 421. Springer, Berlin
178. Brogliato B et al (2002) Numerical simulation of finite dimensional multibody nonsmooth mechanical systems. Appl Mech Rev 55(2):107–150
179. Pfeiffer F (2003) The idea of complementarity in multibody dynamics. Arch Appl Mech 72(11–12):807–816
180. Newton I (1999) The principia: mathematical principles of natural philosophy. University of California Press, Berkeley
181. Jankowski R (2005) Non-linear viscoelastic modelling of earthquake-induced structural pounding. Earthq Eng Struct Dyn 34(6):595–611